



Supplement of

Enhanced photodegradation of dimethoxybenzene isomers in/on ice compared to in aqueous solution

Ted Hullar et al.

Correspondence to: Cort Anastasio (canastasio@ucdavis.edu)

The copyright of individual parts of the supplement might differ from the article licence.

Contents

Supplemental Section S1. Details of light absorption modeling.....	1
Supplemental Section S2. Detailed description of sample preparation methods.....	2
Supplemental Table S1. Experimental light intensity correction factors.....	3
Supplemental Table S2. Light absorbance values.....	4
Supplemental Table S3. Illumination experiment measured parameters.....	11
Supplementary Table S4. Rate constants for light absorption	12
Supplemental Table S5. Machine learning training and testing errors	12
Supplemental Figures S1a-S12h. Results for individual illumination experiments.....	26
Supplemental Figure S13. Experimental and modeled photon fluxes.....	27
Supplemental Figure S14. Light absorbance spectra for DMOB isomers	28
Supplemental Figure S15. Linear decomposition analysis for DMOB isomers	29
Supplemental Figure S16. Action spectra for DMOB light absorbance	31
Supplemental Figure S17. Photodegradation rate constant ratios for shifted absorbance curves.....	32
Supplemental Figure S18. Guaiacol photodegradation rate constants for various illumination conditions.....	33
Supplemental Figure S19. Absorbance spectra for DMOBs compared to assumed Gaussian peaks.....	34
Supplemental Figure S20. Model compound absorbance spectra for various peak locations.....	35
Supplemental Figure S21. Model compound photodegradation rate constants for various peak locations.....	36
Supplemental Figure S22. Model compound absorbance spectra for various peak widths	37
Supplemental Figure S23. Model compound photodegradation rate constants for various peak widths	38
Supplemental Figure S24. Model compound absorbance spectra for various molar absorption coefficients	39
Supplemental Figure S25. Model compound photodegradation rate constant for various molar absorption coefficients	40
Supplemental Figure S26. Machine learning parity plots	41
References	41

Supplemental Section S1. Details of light absorption modeling

Justification for a single machine learning model for all three DMOB isomers. As shown in Supplemental Figure S26 and Supplemental Table S5, the machine learning (ML) model achieves a training R^2 of 0.981 and a testing R^2 of 0.965, along with a training mean absolute error (MAE) of 1.42 nm and a testing MAE of 1.88 nm. Since a universal ML model is fitted to predict the vertical excitation wavelengths (λ) for all three DMOB isomers, we broke down the overall MAE to assess the ML model performance for each molecule. As shown in Supplemental Table S5, the negligible variations in the MAE implies that our model can generate predictions with no bias towards a particular molecule. This trend justified our approach to predict excitation wavelengths for all three molecules using only one ML model. Meanwhile, the overall training and testing MAE for DMOB isomers, as well as the average testing MAE for molecules in solution (1.93 ± 0.16 nm) and at the air-ice interface (1.82 ± 0.23 nm), suggest that this model can be generalized to predict excitation wavelengths for all three isomers in both solution and at the air-ice interface.

Additional information for hyperparameters used to compute Bispectrum Component (BC). Before describing the atomic environment for the three DMOB isomers using a bispectrum component, a set of hyperparameters must be carefully defined. First, the cut-off radius for hydrogen, carbon and oxygen ($R_{cut,H}$, $R_{cut,C}$ & $R_{cut,O}$) are set to 1.5, 2.5, and 3 Å respectively, which corresponds to approximately second-neighbor distances. Meanwhile, to reflect the relative importance for the chemical environment with respect to each atom type, the dimensionless weight factors (ω_H , ω_C & ω_O) of 1.0, 2.0, and 3.0 are set accordingly. Lastly, to ensure a sufficiently large initial feature space for the LASSO model development, a $2j_{max}$ parameter is chosen to be 14, which results in a total of 858 bispectrum components.

Formulation of linear decomposition analysis. To pinpoint the relative importance to the predictions of λ with respect to functional groups of DMOB isomers, a linear decomposition analysis can be performed and formulated as:

$$\lambda_{predicted} = \lambda_0 + \lambda_{predicted,OCH_3} + \lambda_{predicted,C_6H_4}$$

$$\lambda_{Decomposed} = \frac{(\lambda_{predicted,OCH_3} + \lambda_{predicted,C_6H_4})}{\lambda_{predicted} - \lambda_0}$$

In the above equation, λ_0 is the intercept of the LASSO model; $\lambda_{predicted,OCH_3}$ and $\lambda_{predicted,C_6H_4}$ represent predictions contributions from the methoxy groups and from the phenyl ring; and $\lambda_{Decomposed}$ is defined to express the decomposition with respect to the functional groups by percentage.

Supplemental Section S2. Detailed description of sample preparation methods

We placed samples in 10-ml glass beakers (Pyrex, inside diameter 22 mm) and covered them with nylon film (McMaster-Carr, approximately 25 µm thick, secured in place with an o-ring) to reduce evaporation and contamination while allowing sample illumination. As discussed in our previous work with guaiacol (Hullar et al. 2020), we prepared samples using one of five different methods: 1) in an aqueous solution, where we dissolved the test compound in MQ water to give a final concentration of 1.0 µM, then we placed 10 ml of solution in a beaker and covered. 2) Freezer frozen solution, prepared identically to aqueous solution with 10 ml of a 1.0 µM aqueous solution placed in a 10 ml beaker, covered, then placed in a laboratory freezer (-20 °C) for at least 3 hours. 3) Liquid nitrogen frozen solution, which we prepared identically to aqueous solution, then placed it in a pan filled to a depth of 2 cm with liquid nitrogen; sample freezing took approximately 90 seconds. 4) Vapor deposition of gas-phase test compound to the surface of ice. Following an approach previously described (Hullar et al. 2020, Hullar et al. 2018), first we placed 10 ml of MQ water in a beaker, covered it with film, and froze it in a laboratory freezer at -20 °C. We removed and uncovered the frozen samples, and directed a nitrogen stream containing gas-phase dimethoxybenzene at the ice surface for 15 or 30 s. We then recovered the samples and placed them back in a laboratory freezer. 5) Vapor deposited to nature-identical snow, which was produced as described in our previous work (Hullar et al. 2020). We first made nature-identical snow crystals in a custom-built machine derived from previous work (Bones and Adams 2009, Nakamura 1978, Schleef et al. 2014). The snow machine operates in a cold room at -15 °C, nucleates supersaturated water vapor onto nylon wires, forming snow crystals. This snow is then collected and placed in a 500 ml HDPE bottle. To deposit dimethoxybenzene onto the snow, we passed nitrogen from a tank in the cold room first through 500 ml of laboratory-made snow (to condition the nitrogen stream with water vapor), then through a glass container holding 0.4 g of DMOB, and then through a 500-ml HDPE bottle holding the snow to be illuminated, where the DMOB is deposited. 1,2-DMOB is a liquid at room temperature but a solid at -20 °C, while 1,3-DMOB is a liquid at both temperatures and 1,4-DMOB a solid; vapor pressures at 25 °C are 0.057, 0.030, and 0.021 kPa, respectively (USEPA 2021). We then gently mixed the treated snow and transferred it to beakers, tamped it down 10 mm below the top edge of the beaker, and covered it with nylon film.

Supplemental Table S1. Experimental light intensity correction factors. Light intensity correction factors for the experimental illumination system, determined as the ratio of aqueous j_{2NB} in a given position divided by the corresponding value in the reference position (B2). These factors were used to normalize photodegradation rates to the photon flux in each position. Illuminated samples were put in columns B and C, while dark samples (which were uncorrected for photon flux) were placed in columns A and D.

		<u>Column</u>			
		A	B	C	D
<u>Row</u>	1	0.18	1.00	0.80	0.55
	2	0.44	1.00	0.83	0.89
	3	0.61	1.06	0.99	1.10
	4	0.18	1.08	0.95	0.77

Supplemental Table S2. Light absorbance values. Measured, predicted, and modeled light absorbance values for a) 1,2-, b) 1,3-, and c) 1,4-DMOB. Molar absorption coefficients (columns 2 and 4) were measured for aqueous and predicted for the air-ice interface. Modeled absorbance values (columns 5 and 6) were computed using molecular modeling techniques. See footnotes and text for details.

a) 1,2-Dimethoxybenzene

Modeled parameters used to predict air-ice interface spectrum:

Peak wavelength shift from aqueous to air-ice interface: 2.4 nm

Peak height ratio, air-ice interface / aqueous: 1.17

Peak width ratio, air-ice interface / aqueous: 0.94

Wavelength (nm)	Molar absorption coefficient ($M^{-1} \text{ cm}^{-1}$)			Modeled absorbance (AU) ^c	
	Aqueous (measured) ^a	Aqueous (measured) standard error ^a	Air-ice interface (predicted) ^b	Aqueous	Air-ice interface
250	519	0.84	0	0	0
251	572	0.80	0	0	0
252	631	1.34	0	0	0
253	707	0.68	0	0	0
254	795	1.01	613	0	0
255	897	1.21	682	0	0
256	1010	0.80	765	0	0
257	1132	0.85	857	0	0
258	1272	0.79	975	0	0
259	1422	1.18	1113	0	0
260	1585	0.74	1250	0	0
261	1760	1.23	1424	0	0
262	1950	0.81	1610	0	0
263	2153	1.62	1794	0	0
264	2349	1.81	2019	0	0
265	2571	8.27	2258	0.003	0
266	2745	9.05	2497	0.008	0
267	2909	13.44	2749	0.017	0.001
268	3070	13.07	3033	0.031	0.005
269	3236	16.57	3233	0.059	0.016
270	3383	8.75	3445	0.091	0.037
271	3490	13.07	3657	0.150	0.077
272	3564	11.46	3843	0.236	0.112
273	3610	20.29	4019	0.367	0.155
274	3594	9.20	4134	0.556	0.263
275	3498	15.85	4219	0.755	0.439
276	3337	19.54	4227	1.022	0.632
277	3196	14.64	4133	1.375	0.813
278	3109	16.90	3958	1.662	1.026
279	3043	7.75	3772	1.859	1.276
280	2883	7.66	3641	2.050	1.552

281	2486	3.20	3566	2.096	1.886
282	1960	3.23	3373	2.008	2.137
283	1415	3.33	2846	1.995	2.273
284	978	2.34	2229	1.994	2.386
285	649	1.26	1549	1.843	2.452
286	434	0.81	1014	1.612	2.422
287	284	0.45	677	1.410	2.260
288	186	0.62	426	1.240	2.014
289	117	0.39	271	1.035	1.753
290	75	0.97	174	0.823	1.459
291	47	1.00	105	0.623	1.167
292	30	0.31	63	0.439	0.937
293	19	0.79	40	0.301	0.717
294	12	1.29	24	0.211	0.477
295	8.17	0.51	15	0.147	0.296
296	5.35	0.55	10	0.098	0.202
297	3.40	0.47	6.26	0.072	0.156
298	2.15	0.80	3.81	0.065	0.116
299	1.37	0.86	2.42	0.056	0.072
300	0.87	0.97	1.47	0.040	0.046
301	0.55	0.47	0.89	0.028	0.031
302	0.35	0.73	0.57	0.022	0.016
303	0.22	0.58	0.34	0.017	0.005
304	0.14	0.93	0.21	0.011	0.001
305	0.089	0.37	0.13	0.005	0
306	0.057	0.99	0.080	0.002	0
307	0.036	0.93	0.048	0.000	0
308	0.023	0.67	0.031	0.001	0
309	0.014	0.30	0.019	0.004	0
310	0.0092	0.87	0.011	0.005	0
311	0.0058	0.40	0.0072	0.003	0
312	0.0037	0.44	0.0043	0.001	0
313	0.0023	0.67	0.0026	0	0
314	0.0015	0.75	0.0017	0	0
315	0.00094	0.69	0.0010	0	0
316	0.00060	0.44	0.00062	0	0

b) 1,3-Dimethoxybenzene

Modeled parameters used to predict air-ice interface spectrum:

Peak wavelength shift from aqueous to air-ice interface: 5.2 nm

Peak height ratio, air-ice interface / aqueous: 0.91

Peak width ratio, air-ice interface / aqueous: 1.27

Wavelength (nm)	Molar absorption coefficient (M ⁻¹ cm ⁻¹)			Modeled absorbance (AU) ^c	
	Aqueous (measured) ^a	Aqueous (measured) standard error ^a	Air-ice interface (predicted) ^b	Aqueous	Air-ice interface
250	536	2.20	522	0	0
251	600	2.25	571	0	0
252	670	2.72	626	0	0
253	758	2.34	690	0	0
254	853	2.00	758	0	0
255	967	2.70	836	0	0
256	1098	2.25	925	0	0
257	1235	2.61	1023	0	0
258	1395	2.99	1111	0	0
259	1558	3.04	1225	0	0
260	1745	2.67	1343	0	0
261	1938	2.52	1464	0	0.001
262	2158	3.41	1606	0.002	0.004
263	2393	3.15	1747	0.008	0.005
264	2570	43.20	1903	0.012	0.004
265	2796	32.11	2070	0.027	0.006
266	2984	33.64	2215	0.066	0.015
267	3165	39.48	2339	0.122	0.024
268	3322	35.39	2504	0.160	0.040
269	3494	33.04	2646	0.226	0.084
270	3663	39.52	2780	0.356	0.127
271	3859	41.74	2914	0.510	0.139
272	3997	45.15	3023	0.624	0.192
273	4010	45.44	3148	0.789	0.288
274	3889	43.95	3272	1.035	0.422
275	3638	47.63	3407	1.258	0.579
276	3443	35.54	3526	1.423	0.725
277	3385	32.08	3627	1.582	0.843
278	3476	35.40	3653	1.683	0.986
279	3479	30.13	3607	1.742	1.179
280	3190	40.92	3470	1.718	1.315
281	2592	44.15	3290	1.592	1.422
282	1867	2.10	3149	1.513	1.505
283	1260	2.44	3091	1.464	1.551
284	844	2.76	3112	1.318	1.570
285	541	2.36	3178	1.109	1.586
286	348	1.82	3166	0.903	1.590

287	224	2.14	2976	0.741	1.545
288	142	2.15	2603	0.595	1.439
289	89	1.90	2076	0.454	1.276
290	56	1.75	1584	0.347	1.140
291	36	1.88	1147	0.254	1.020
292	22	1.77	839	0.183	0.884
293	13	1.91	586	0.130	0.755
294	8.3	1.17	433	0.095	0.648
295	5.3	1.62	304	0.067	0.545
296	2.9	1.74	213	0.040	0.432
297	1.8	1.54	150	0.023	0.346
298	1.2	1.26	104	0.016	0.280
299	0.72	1.89	71	0.015	0.223
300	0.45	1.79	49	0.012	0.189
301	0.28	1.50	34	0.007	0.159
302	0.18	2.08	23	0.003	0.122
303	0.11	1.79	16	0.001	0.087
304	0.069	2.01	11	0	0.061
305	0.043	1.98	7.5	0	0.044
306	0.027	2.04	5.2	0	0.036
307	0.017	1.13	3.4	0	0.029
308	0.011	1.64	2.2	0	0.021
309	0.0067	0.98	1.5	0	0.016
310	0.0042	1.41	1.0	0	0.013
311	0.0026	1.87	0.73	0	0.010
312	0.0016	1.92	0.52	0	0.006
313	0.0010	0.97	0.36	0	0.003
314	0.00064	1.72	0.25	0	0.002
315	0.00040	0.81	0.17	0	0.002
316	0		0.12	0	0.001
317	0		0.080	0	0
318	0		0.055	0	0
319	0		0.038	0	0
320	0		0.026	0	0
321	0		0.019	0	0
322	0		0.013	0	0
323	0		0.0089	0	0
324	0		0.0061	0	0
325	0		0.0042	0	0
326	0		0.0029	0	0
327	0		0.0020	0	0
328	0		0.0014	0	0
329	0		0.00093	0	0
330	0		0.00068	0	0
331	0		0.00046	0	0
332	0		0.00015	0	0

c) 1,4-Dimethoxybenzene

Modeled parameters used to predict air-ice interface spectrum:

Peak wavelength shift from aqueous to air-ice interface: 1.6 nm

Peak height ratio, air-ice interface / aqueous: 1.06

Peak width ratio, air-ice interface / aqueous: 0.92

Wavelength (nm)	Molar absorption coefficient ($M^{-1} cm^{-1}$)			Modeled absorbance (AU) ^c	
	Aqueous (measured) ^a	Aqueous (measured) standard error ^a	Air-ice interface (predicted) ^b	Aqueous	Air-ice interface
250	167	1.08	0	0	0
251	163	0.80	0	0	0
252	165	0.78	0	0	0
253	171	0.90	0	0	0
254	181	1.24	0	0	0
255	197	0.81	176	0	0
256	216	1.14	174	0	0
257	238	1.13	178	0	0
258	267	1.07	187	0	0
259	298	0.64	201	0	0
260	336	1.36	222	0	0
261	379	1.43	247	0	0
262	428	1.15	280	0	0
263	482	1.34	316	0	0
264	540	2.01	361	0	0
265	603	2.33	411	0	0
266	667	2.78	471	0	0
267	739	2.63	536	0	0
268	819	3.53	602	0	0
269	895	2.57	681	0	0
270	975	3.04	760	0	0
271	1060	3.76	843	0	0
272	1149	4.06	933	0	0
273	1244	4.71	1025	0	0
274	1341	4.73	1124	0	0
275	1446	4.90	1227	0	0
276	1552	5.16	1338	0	0
277	1655	5.55	1456	0	0
278	1755	6.39	1581	0	0
279	1851	5.56	1696	0	0
280	1947	6.34	1820	0.002	0
281	2026	6.66	1932	0.002	0
282	2119	7.15	2044	0.001	0
283	2192	6.64	2131	0.000	0
284	2251	7.24	2236	0.002	0
285	2302	8.09	2324	0.006	0
286	2321	7.13	2393	0.009	0
287	2326	7.94	2441	0.016	0

288	2314	7.61	2469	0.024	0
289	2276	6.80	2466	0.036	0
290	2221	7.56	2434	0.053	0.002
291	2150	6.80	2380	0.081	0.008
292	2072	7.00	2305	0.114	0.014
293	1983	6.56	2214	0.137	0.018
294	1875	5.49	2110	0.181	0.028
295	1761	5.73	2000	0.275	0.066
296	1633	5.77	1867	0.379	0.132
297	1472	4.95	1714	0.475	0.211
298	1301	4.19	1525	0.577	0.312
299	1114	3.89	1320	0.700	0.428
300	917	3.03	1093	0.866	0.551
301	727	2.42	870	1.068	0.716
302	554	2.16	662	1.302	0.917
303	415	1.50	482	1.528	1.133
304	303	1.08	345	1.683	1.381
305	221	0.83	242	1.784	1.601
306	157	1.03	166	1.885	1.798
307	109	0.16	115	1.993	1.990
308	74	0.98	76	2.034	2.086
309	52	0.49	51	1.959	2.131
310	35	0.88	33	1.788	2.145
311	25	0.58	22	1.610	2.058
312	17	0.71	16	1.486	1.883
313	13	0.57	11	1.361	1.654
314	8.8	0.49	7.22	1.204	1.418
315	6.1	0.40	4.83	1.039	1.216
316	4.2	0.61	3.22	0.873	1.048
317	2.9	0.25	2.15	0.713	0.873
318	2.0	0.62	1.44	0.560	0.701
319	1.4	0.35	1.00	0.421	0.550
320	1.0	1.23	0.67	0.309	0.415
321	0.67	1.13	0.45	0.225	0.296
322	0.47	0.94	0.30	0.166	0.199
323	0.32	1.44	0.20	0.124	0.139
324	0.22	0.85	0.13	0.085	0.104
325	0.16	0.90	0.089	0.053	0.073
326	0.11	0.97	0.059	0.032	0.047
327	0.075	0.51	0.040	0.017	0.030
328	0.052	0.78	0.026	0.010	0.018
329	0.036	0.29	0.018	0.006	0.010
330	0.025	0.52	0.012	0.004	0.007
331	0.017	0.98	0.0082	0.003	0.005
332	0.012	0.62	0.0055	0.002	0.002
333	0.0083	1.14	0.0037	0.001	0.001
334	0.0057	0.53	0.0024	0	0
335	0.0040	0.64	0.0016	0	0

336	0.0028	0.77	0.0011	0	0
337	0.0019	0.14	0.00073	0	0
338	0.0013	0.49	0.00049	0	0
339	0.00092	0.96	0	0	0
340	0.00064	0.53	0	0	0
341	0.00044	0.47	0	0	0

^a For each DMOB, we measured absorbance spectra in five aqueous solutions (10-1000 μ M) at 25 °C using a UV-2501PC spectrophotometer (Shimadzu) in 1.0 cm cuvettes against a MQ reference cell. For each wavelength, we calculated the base-10 molar absorption coefficient as the slope of the linear regression of measured absorbance versus the DMOB concentration. Standard errors are the SE of the slope of the regression line. At wavelengths from 296-316, 296-315, and 313-341 nm for 1,2-, 1,3-, and 1,4-DMOB respectively, the calculated molar absorption coefficients were <5 M⁻¹ cm⁻¹ and very noisy. To better estimate molar absorption coefficients in these ranges, we used the measured data from 290-296, 290-296, and 307-313 nm for each compound respectively, plotted λ vs $\ln(\epsilon_{\text{DMOB},\lambda})$, then used the slope of the linear regression to determine $\epsilon_{\text{DMOB},\lambda}$ at wavelengths longer than these ranges.

^b Predicted molar absorption coefficients at the air-ice interface, based on aqueous absorbance values adjusted using modeled absorbance changes between solution and the air-ice interface. See text for details.

^c Results of computationally-determined absorbance spectra in aqueous solution and at the air-ice interface in arbitrary absorbance units. See text for details.

Supplemental Table S3. Illumination experiment measured parameters. Summary of parameters determined from illumination experiments, summarized for each DMOB isomer and experimental condition. “avg” represents the mean value for each isomer and sample treatment, “SD” is the standard deviation, and “95% CI” is the 95 percent confidence interval of the mean.

n ^a	$j_{\text{DMOB}} (\text{min}^{-1})$ ^b			$k'_{\text{DMOB, dark}} (\text{min}^{-1})$ ^c			$j_{\text{DMOB,exp}} (\text{min}^{-1})$ ^d			$j^*_{\text{DMOB}} (\text{min}^{-1}/\text{s}^{-1})$ ^e			$j_{\text{2NB}} (\text{s}^{-1})$ ^f			
	avg	SD	95% CI	avg	SD	95% CI	avg	SD	95% CI	avg	SD	95% CI	avg	SD	95% CI	
1,2-DMOB																
Aqueous	3	9.3E-06	4.7E-06	1.2E-05	3.5E-06	2.2E-06	5.5E-06	5.8E-06	3.1E-06	7.8E-06	1.9E-03	1.1E-03	2.7E-03	3.2E-03	2.7E-04	6.6E-04
Freezer frozen solution	3	-4.8E-06	2.9E-05	7.1E-05	-4.9E-05	1.6E-05	3.9E-05	-4.8E-06	2.9E-05	7.1E-05	-1.5E-03	9.9E-03	2.5E-02	2.9E-03	1.8E-04	4.5E-04
Liquid nitrogen frozen solution	4	5.0E-06	7.8E-06	1.2E-05	-1.1E-06	2.8E-06	4.4E-06	4.5E-06	7.9E-06	1.3E-05	1.9E-03	3.4E-03	5.4E-03	2.6E-03	1.9E-04	3.0E-04
Vapor-deposited to ice surface	3	1.8E-04	1.7E-04	4.2E-04	2.1E-05	2.3E-05	5.7E-05	1.5E-04	1.6E-04	4.0E-04	2.9E-02	2.2E-02	5.5E-02	5.2E-03	2.6E-03	6.5E-03
Vapor-deposited to snow	5	4.3E-05	1.5E-05	1.9E-05	-2.1E-06	2.8E-05	3.5E-05	3.3E-05	9.9E-06	1.2E-05	2.7E-02	8.4E-03	1.0E-02	1.2E-03	3.1E-05	3.9E-05
1,3-DMOB																
Aqueous	6	1.1E-05	1.0E-05	1.1E-05	1.5E-05	1.4E-05	1.5E-05	-3.4E-06	9.1E-06	9.5E-06	-1.1E-03	2.9E-03	3.0E-03	3.3E-03	2.1E-04	2.2E-04
Freezer frozen solution	0															
Liquid nitrogen frozen solution	3	2.8E-05	7.9E-06	2.0E-05	-1.1E-07	2.3E-06	5.7E-06	2.8E-05	9.0E-06	2.2E-05	1.3E-02	4.2E-03	1.1E-02	2.1E-03	3.8E-05	9.6E-05
Vapor-deposited to ice surface	0															
Vapor-deposited to snow	5	2.2E-04	5.1E-05	6.3E-05	1.6E-04	3.7E-05	4.6E-05	6.2E-05	4.9E-05	6.1E-05	5.4E-02	4.5E-02	5.6E-02	1.2E-03	7.4E-05	9.2E-05
1,4-DMOB																
Aqueous	3	2.0E-05	6.3E-06	1.6E-05	7.1E-06	6.0E-06	1.5E-05	1.3E-05	2.7E-06	6.7E-06	4.3E-03	7.3E-04	1.8E-03	3.1E-03	1.2E-04	3.0E-04
Freezer frozen solution	0															
Liquid nitrogen frozen solution	3	4.5E-05	3.4E-06	8.5E-06	-2.3E-07	8.2E-06	2.0E-05	4.3E-05	6.2E-06	1.5E-05	1.5E-02	3.6E-03	9.0E-03	3.0E-03	5.2E-04	1.3E-03
Vapor-deposited to ice surface	5	1.1E-04	7.1E-05	8.8E-05	5.5E-05	4.7E-05	5.9E-05	5.2E-05	9.5E-05	1.2E-04	1.4E-02	2.5E-02	3.1E-02	4.2E-03	5.6E-04	6.9E-04
Vapor-deposited to snow	8	4.2E-04	2.7E-04	2.2E-04	2.2E-04	2.4E-04	2.0E-04	2.0E-04	1.7E-04	1.4E-04	1.1E-01	9.1E-02	7.6E-02	1.6E-03	6.9E-04	5.8E-04

^a Number of experiments

^b The pseudo-first-order rate constant for DMOB loss during sample illumination, obtained as the slope of $\ln([DMOB]_t/[DMOB]_0)$ vs t, where $[DMOB]_t$ was corrected for variations in light flux at each illumination position

^c Rate constant for DMOB loss in dark controls

^d Dark-corrected experimental photodegradation rate constant, obtained by subtracting $k'_{\text{DMOB, dark}}$ from j_{DMOB}

^e Photon flux-normalized photodegradation rate constant, normalized by dividing the dark-corrected experimental photodegradation rate constant ($j_{\text{DMOB,exp}}$) by the daily measured j_{2NB} value

^f Daily measured 2NB photolysis rate constant, measured using the same sample preparation method as the DMOB sample, except in the case of snow samples. For snow samples, j_{2NB} was measured in aqueous solution and multiplied by previously determined correction factor of 0.38 to give a snow j_{2NB} value

Supplementary Table S4. Rate constants for light absorption. Integrated rate constants for light absorption, determined for each DMOB isomer by multiplying the measured (aqueous) or predicted (air-ice interface) molar absorption coefficient by the experimental or Summit conditions photon flux, then summing the resulting values. Ratios for each isomer are the air-ice interface rate constant divided by the aqueous rate constant.

Compound	Experimental light conditions			Summit light conditions		
	Rate constant for light absorption ^a (photons molecule ⁻¹ s ⁻¹)		Rate constant ratio Air-ice interface/ aqueous	Rate constant for light absorption ^a (photons molecule ⁻¹ s ⁻¹)		Rate constant ratio Air-ice interface/ aqueous
	Aqueous	Air-ice interface		Aqueous	Air-ice interface	
1,2-DMOB	6.8E-06	1.2E-05	1.7	3.4E-08	5.1E-08	1.5
1,3-DMOB	6.5E-06	3.4E-05	5.3	1.7E-08	2.8E-06	170
1,4-DMOB	1.0E-04	1.2E-04	1.1	8.1E-05	8.3E-05	1.0

^a Calculated using $\Sigma (2303/N_A I_\lambda \epsilon_\lambda)$, where 2303 is a factor for units and base conversion ($1000 \text{ cm}^3 \text{ L}^{-1}$), N_A is Avogadro's number ($6.022 \times 1023 \text{ molecules mol}^{-1}$), I_λ is the experimental or modeled photon flux at each wavelength (photons $\text{cm}^{-2} \text{ s}^{-1} \text{ nm}^{-1}$), and ϵ_λ is the wavelength-dependent molar absorptivity for each DMOB ($\text{M}^{-1} \text{ cm}^{-1}$).

Supplemental Table S5. Machine learning training and testing errors. Summary of training and testing Mean Absolute Error (MAE) for each DMOB molecule in the machine learning model of light absorption. Both the training and the testing MAE are computed by averaging the MAE from the 5-fold cross validation scheme.

Summary of mean absolute error (MAE) from the ML model		
	Training MAE (nm)	Testing MAE (nm)
1,2-DMOB	1.38	1.84
1,3-DMOB	1.39	1.92
1,4-DMOB	1.50	1.87
Average & Std	1.42 ± 0.056	1.88 ± 0.031

Figure S1a. 12DMOB (0.96 μ M), aqueous 20180215 Aqueous

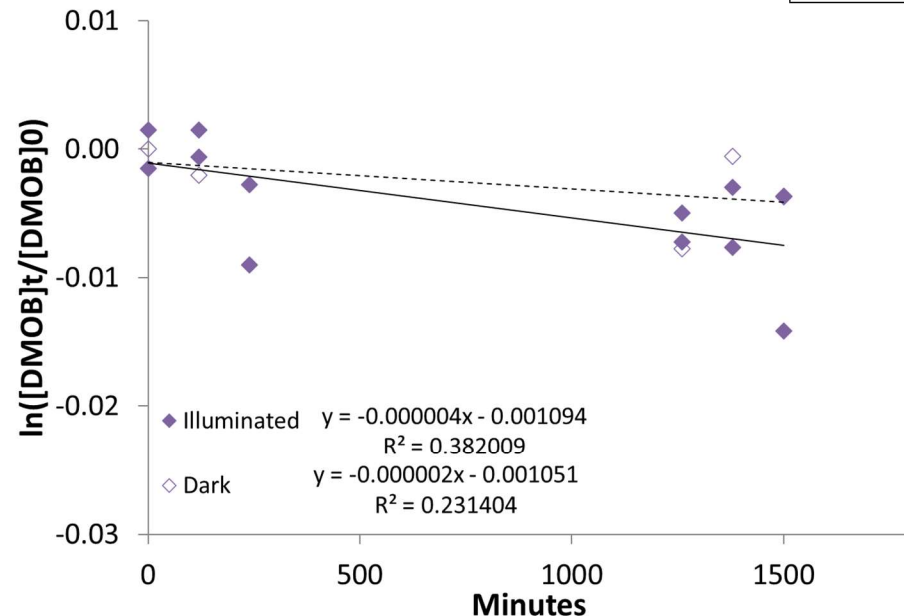


Figure S1b. 12DMOB (0.98 μ M), aqueous 20180308 Aqueous

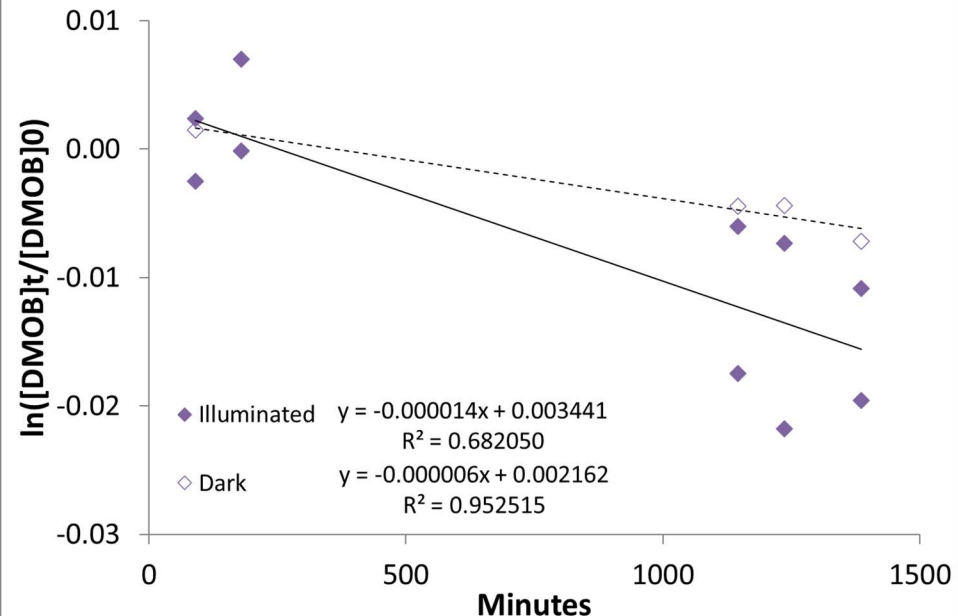


Figure S1c. 1,2-DMOB (0.97 μ M), aqueous 20180321 Aqueous

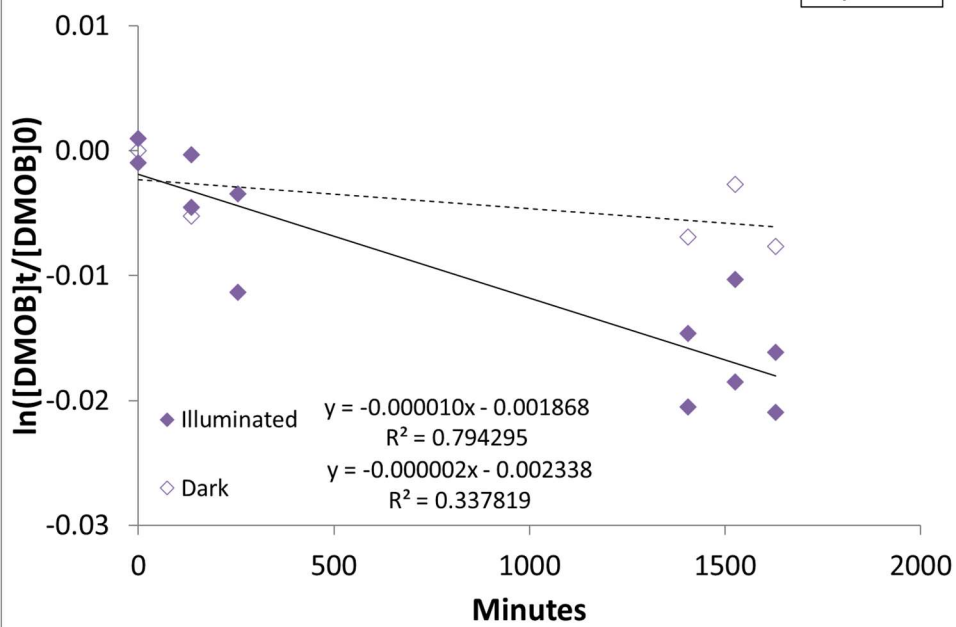


Figure S2a. 1,2-DMOB (0.88 μ M), frozen solution 20180420

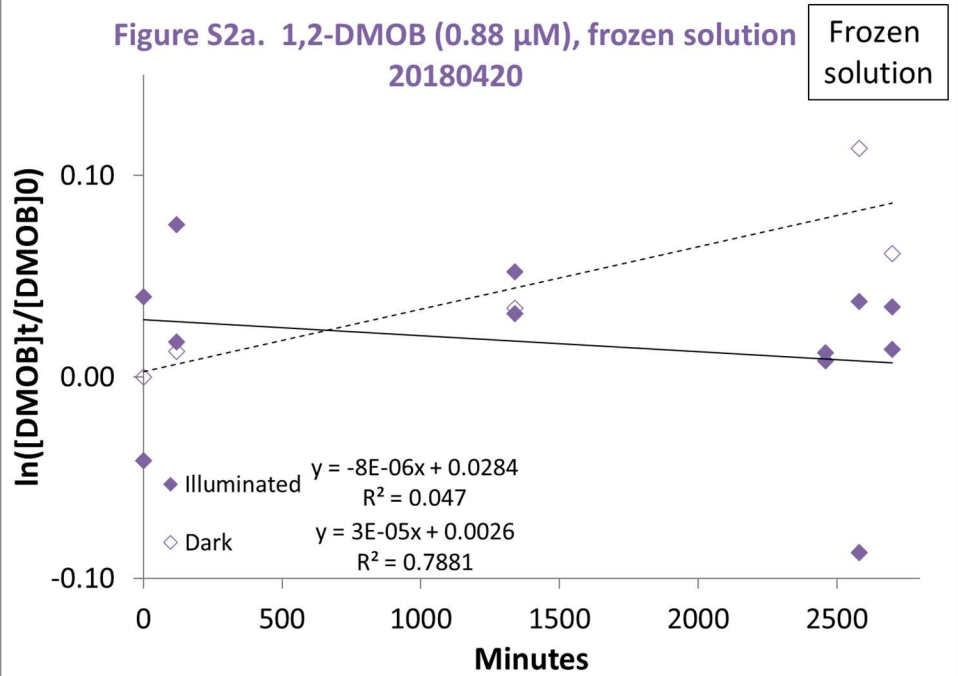


Figure S2b. 1,2-DMOB (0.94 μ M), frozen solution

Frozen solution

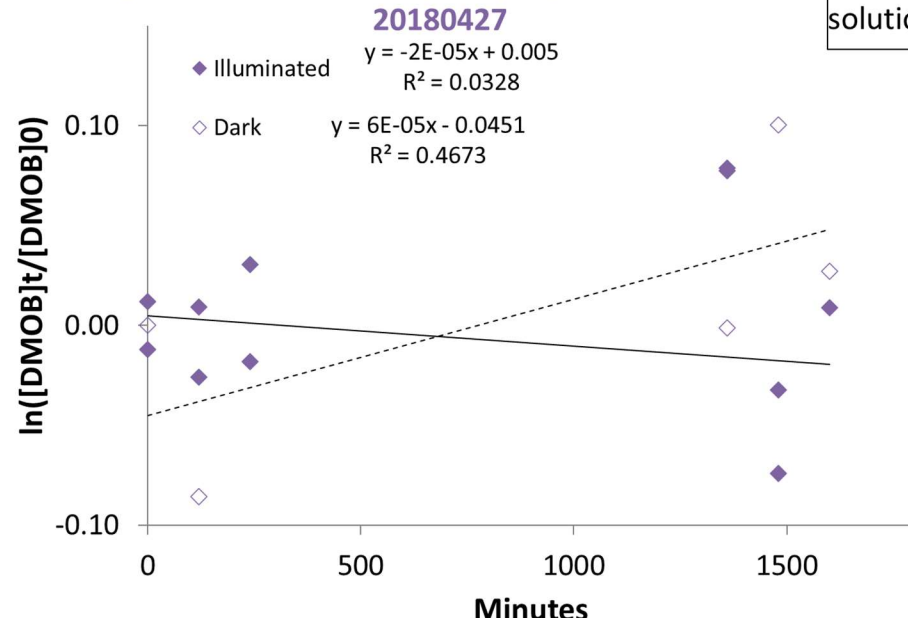


Figure S2c. 1,2-DMOB (0.85 μ M), frozen solution

Frozen solution

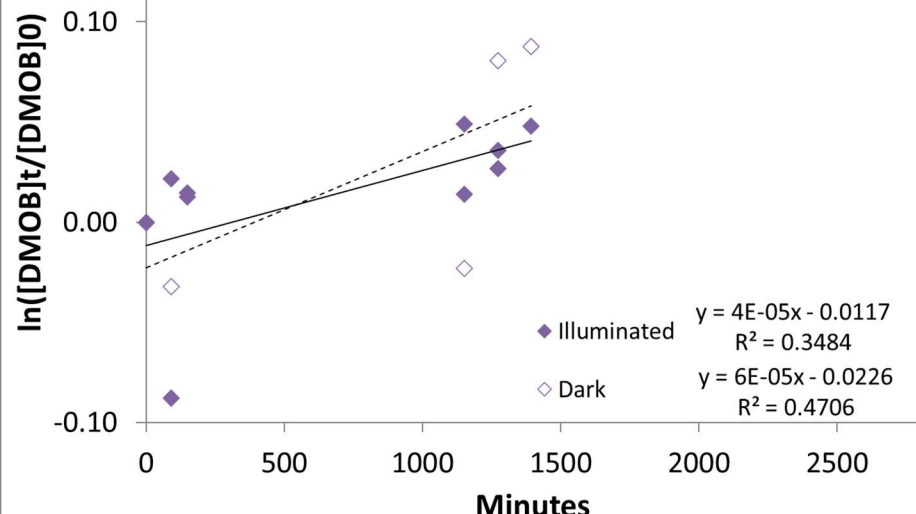


Figure S3a. 1,2-DMOB (0.93 μ M), LN2 20180920

LN2

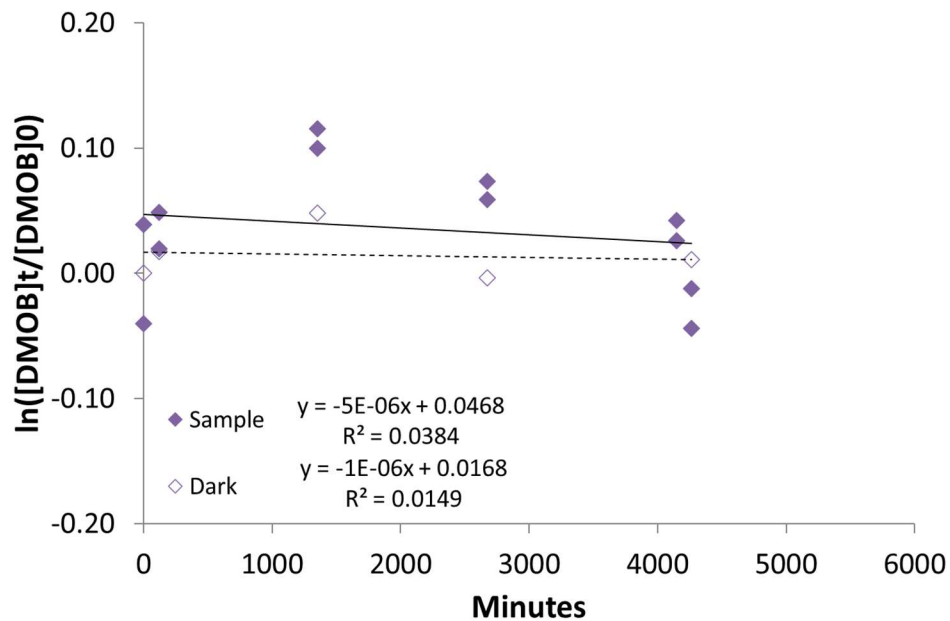


Figure S3b. 1,2-DMOB (1.0 μ M), LN2 20180928

LN2

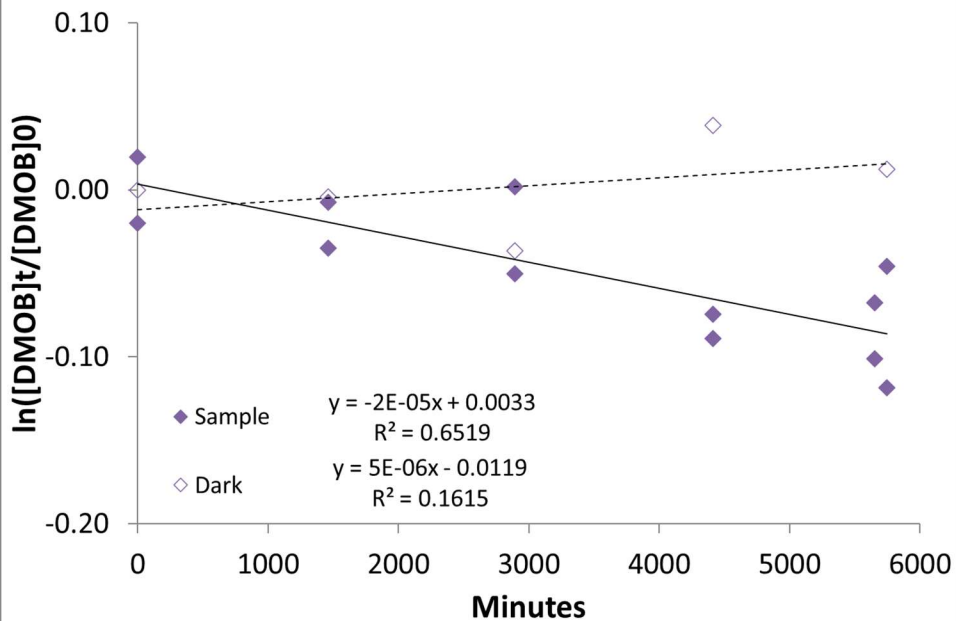
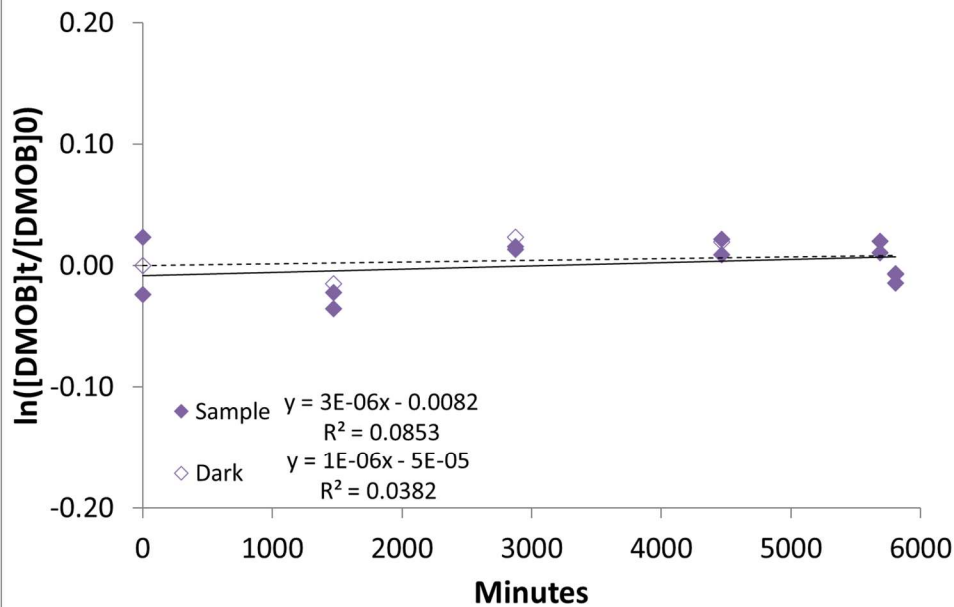


Figure S3c. 1,2-DMOB (1.0 μ M), LN2 20181013

LN2

Figure S3d. 1,2-DMOB (1.0 μ M), LN2 20181026

LN2

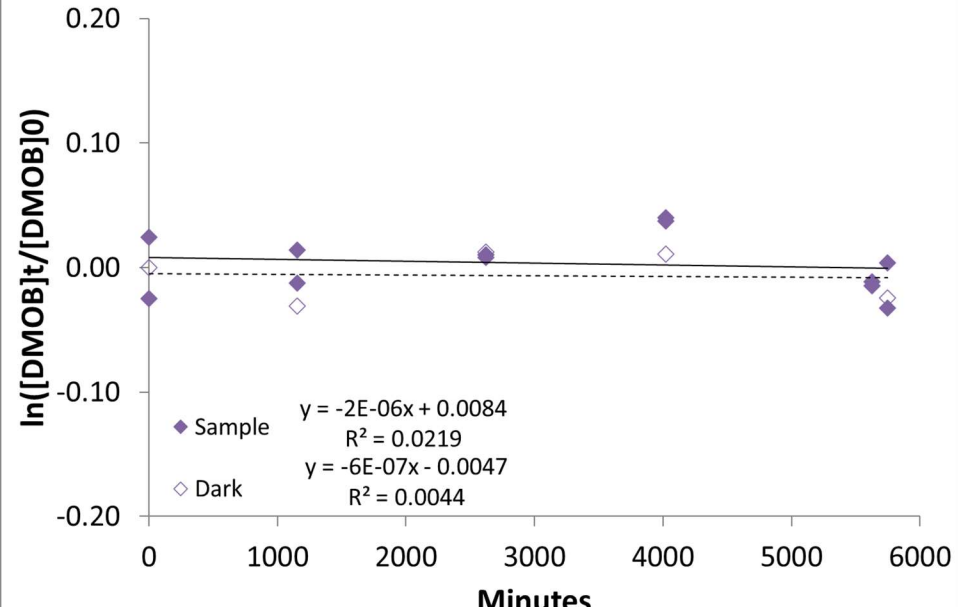
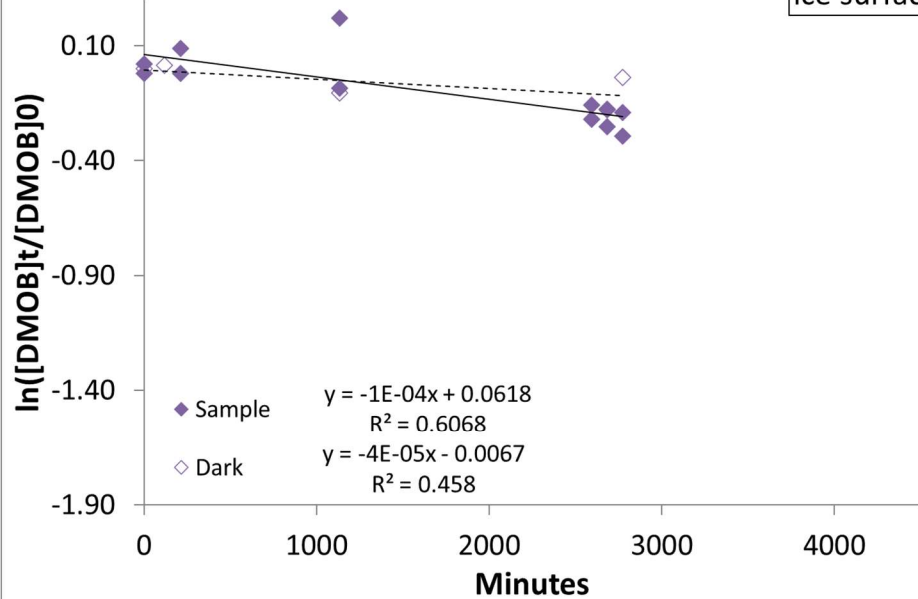
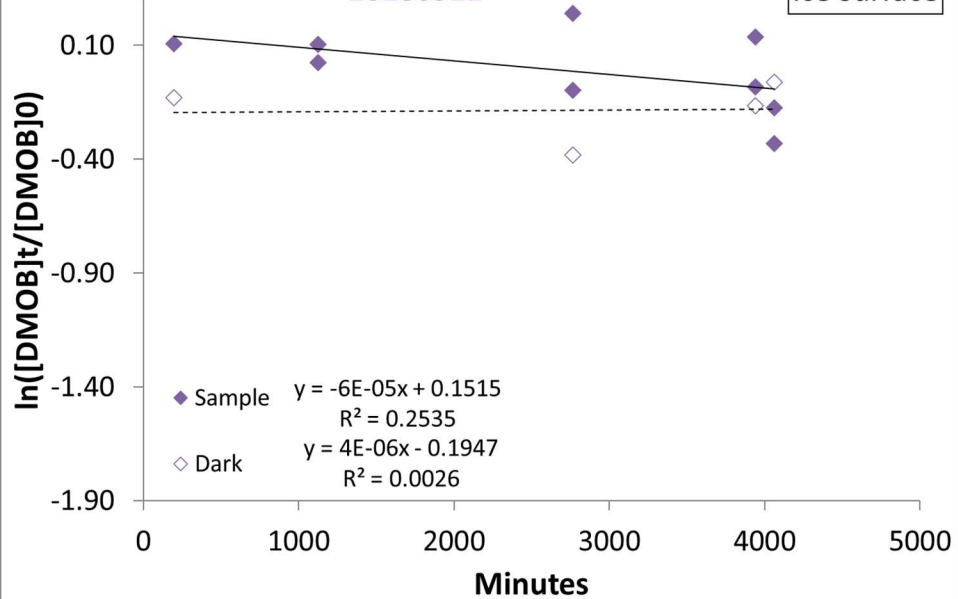
Figure S4a. 1,2-DMOB (17 μ M), VD to ice surface
20180503VD to
ice surfaceFigure S4b. 1,2-DMOB (3.0 μ M), VD to ice surface
20180511VD to
ice surface

Figure S4c. 1,2-DMOB (4.3 μ M), VD to ice surface
20180621

VD to
ice surface

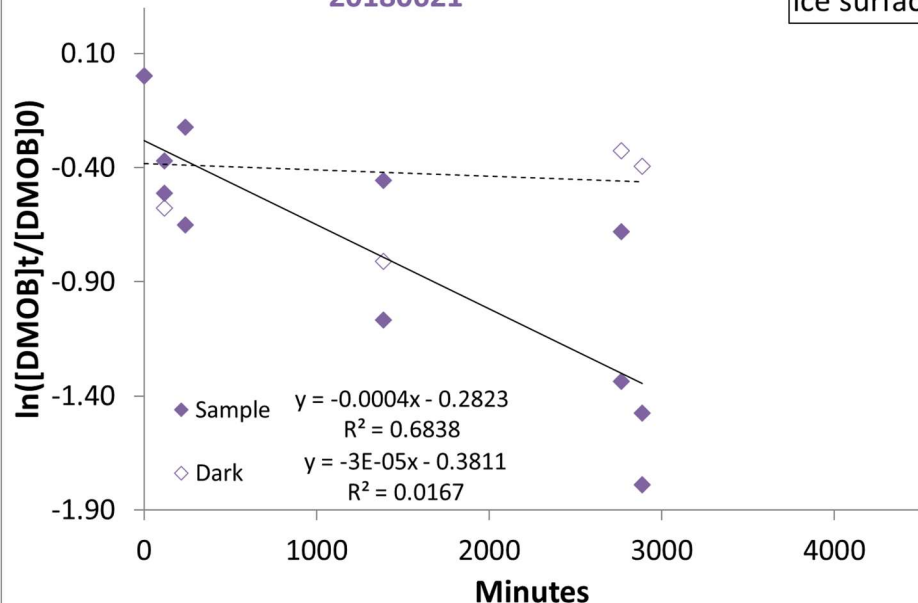


Figure S5a. 1,2-DMOB (0.40 μ M), VD to snow
20180206

VD to
snow

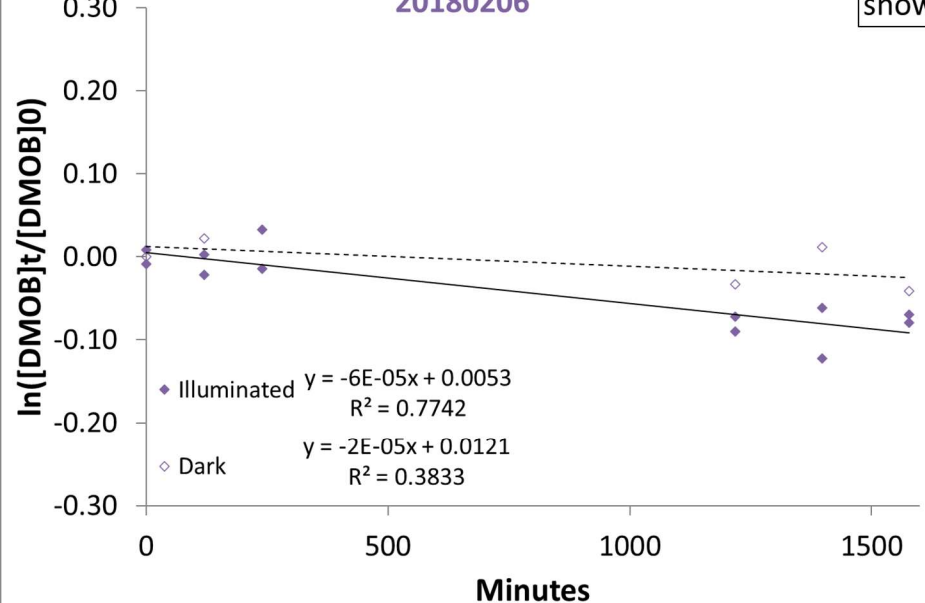


Figure S5b. 1,2-DMOB (1.8 μ M), VD to snow
20180314

VD to
snow

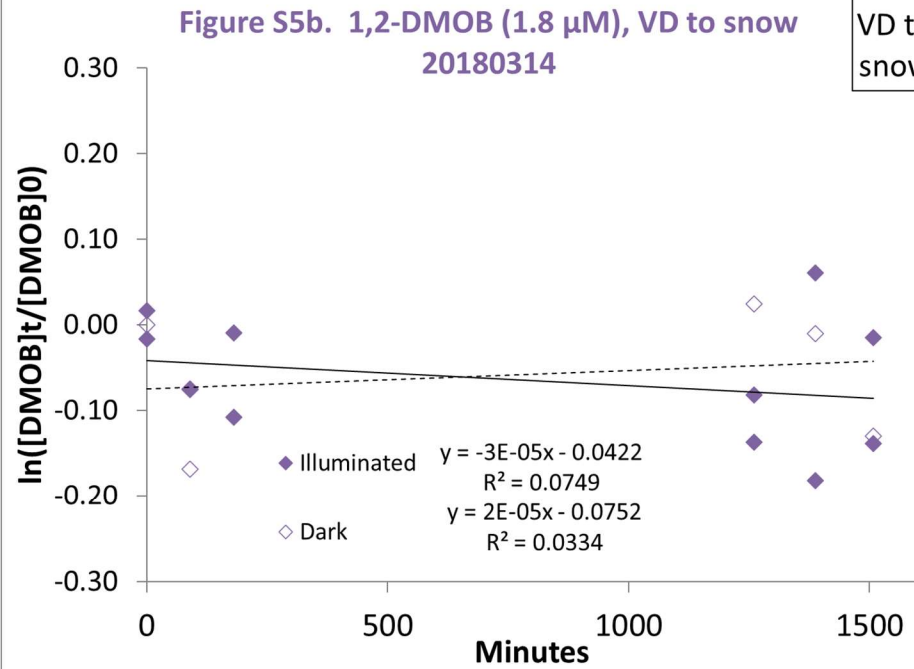
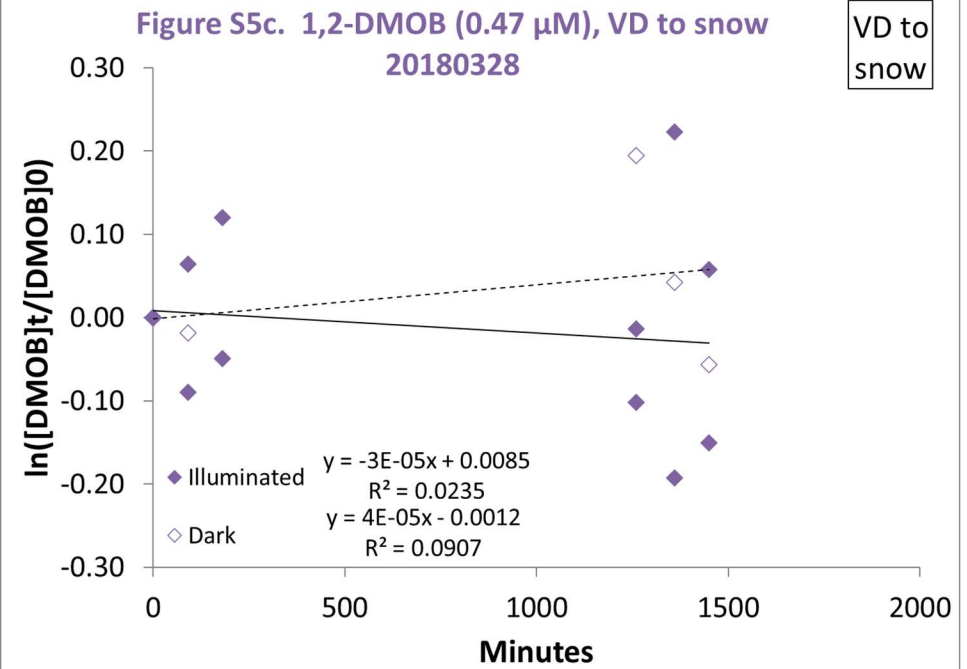


Figure S5c. 1,2-DMOB (0.47 μ M), VD to snow
20180328

VD to
snow



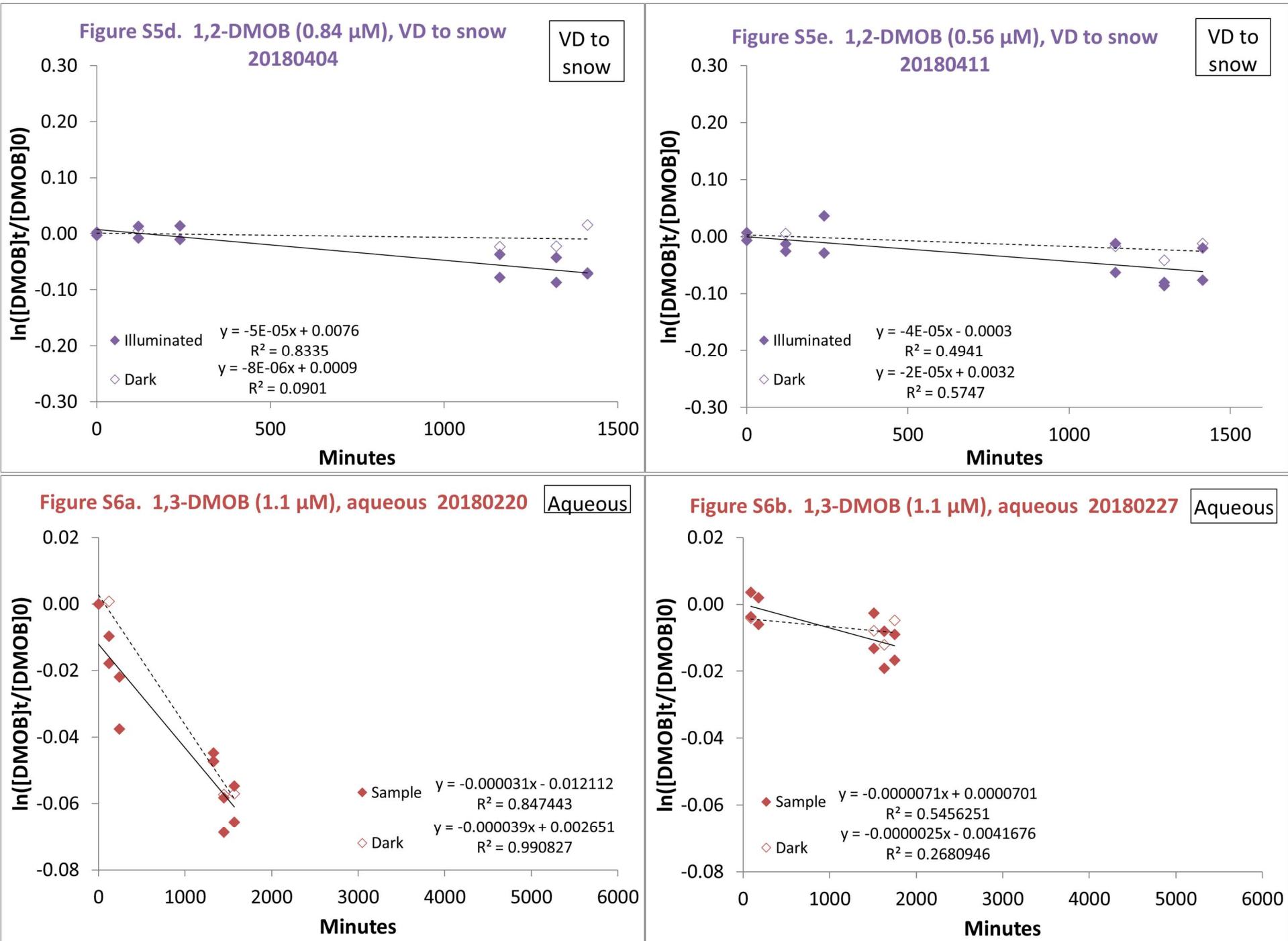


Figure S6c. 1,3-DMOB (1.2 μ M), aqueous 20180329 Aqueous

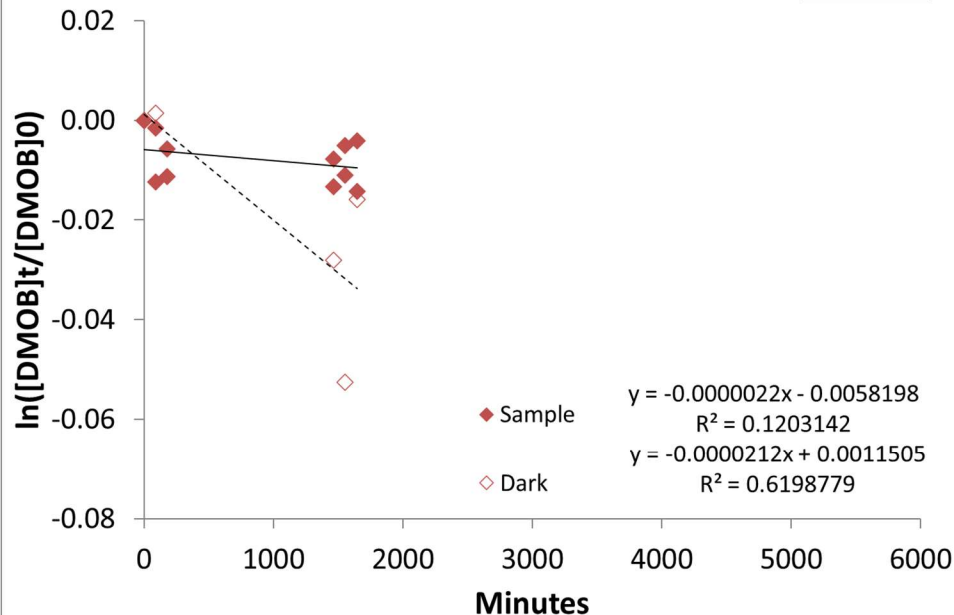


Figure S6d. 1,3-DMOB (1.0 μ M), aqueous 20180413 Aqueous

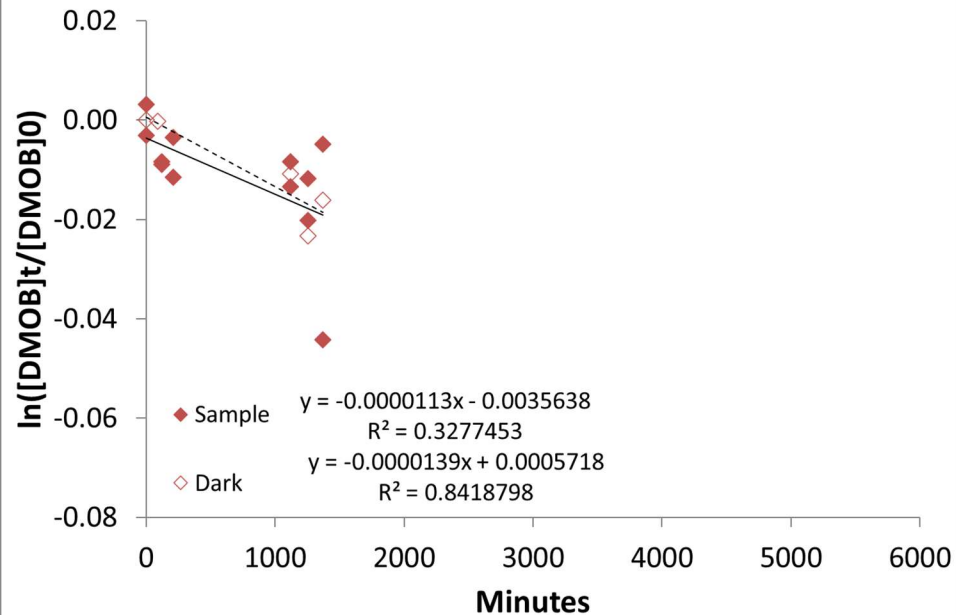


Figure S6e. 1,3-DMOB (1.0 μ M), aqueous 20180702 Aqueous

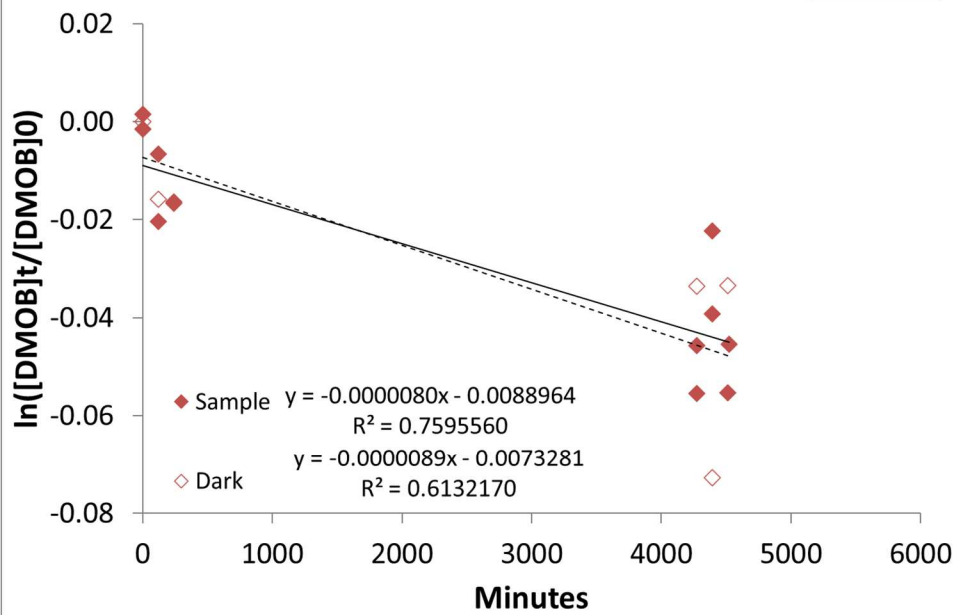


Figure S6f. 1,3-DMOB (1.0 μ M), aqueous 20181103 Aqueous

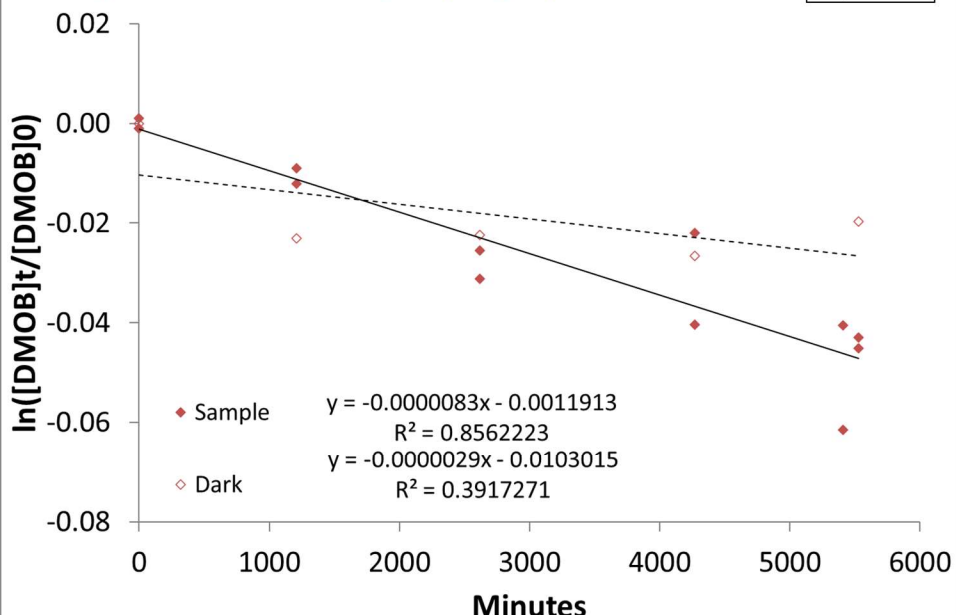


Figure S7a. 1,3-DMOB (0.90 μ M), LN2 20181109

LN2

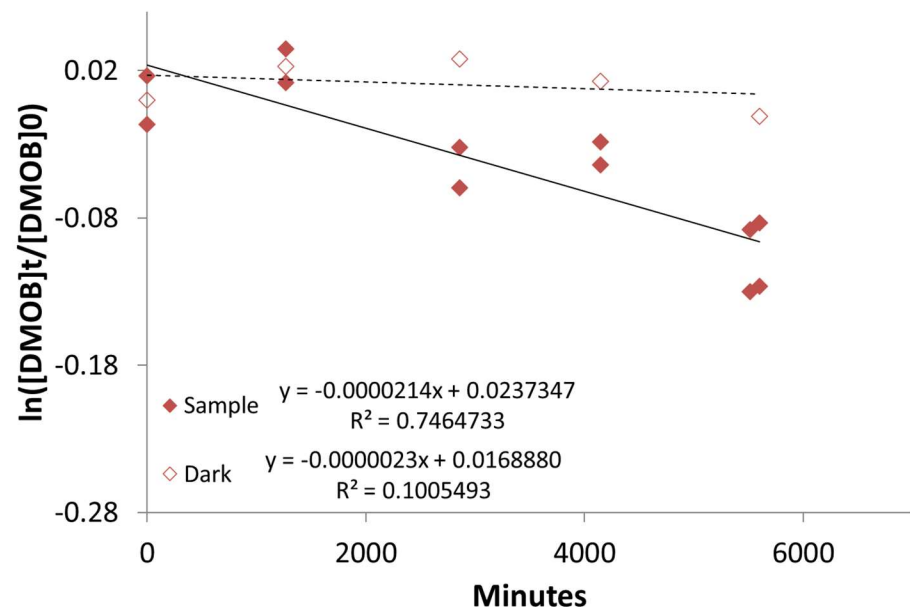


Figure S7b. 1,3-DMOB (0.93 μ M), LN2 20181208

LN2

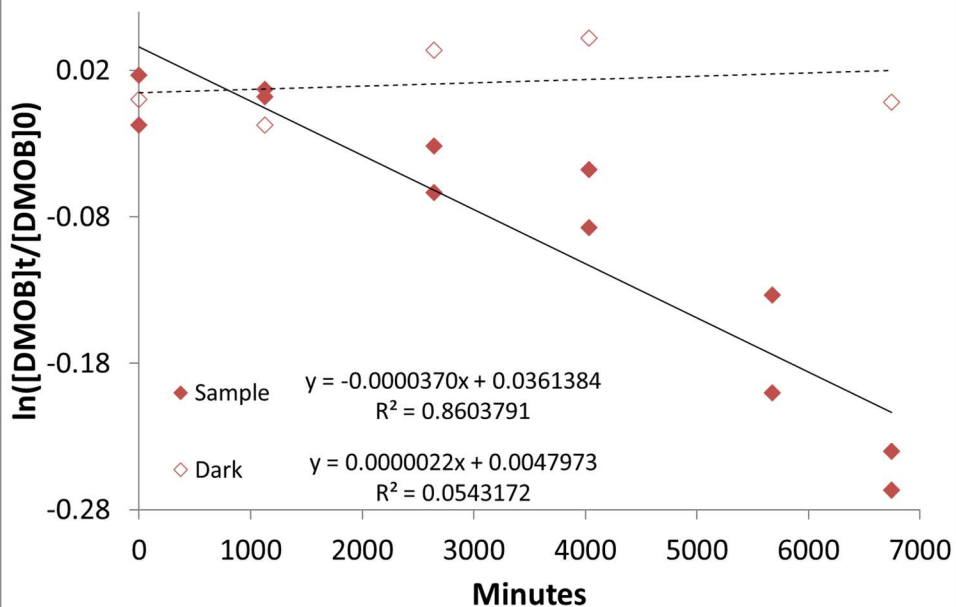


Figure S7c. 1,3-DMOB (0.94 μ M), LN2 20181130

LN2

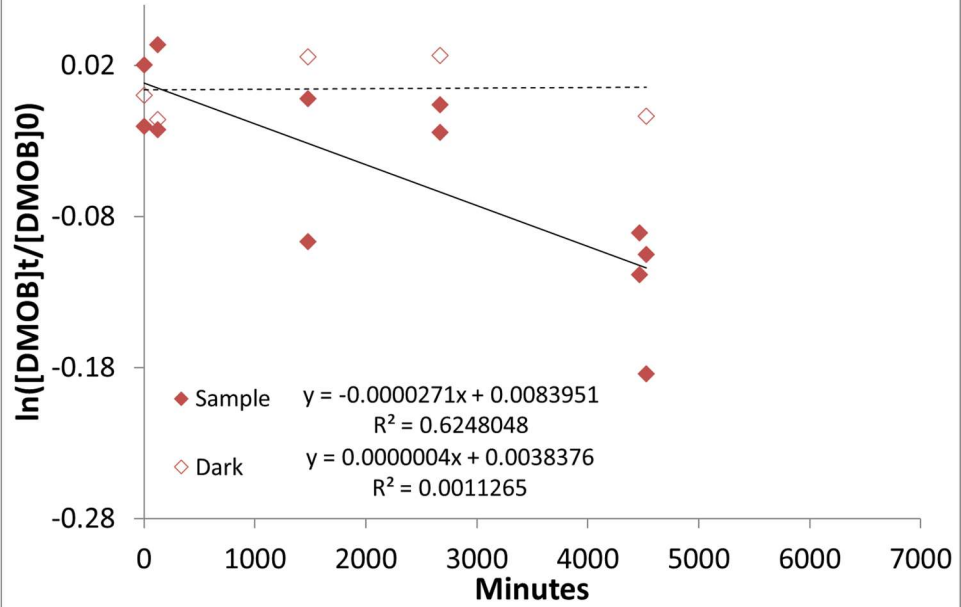
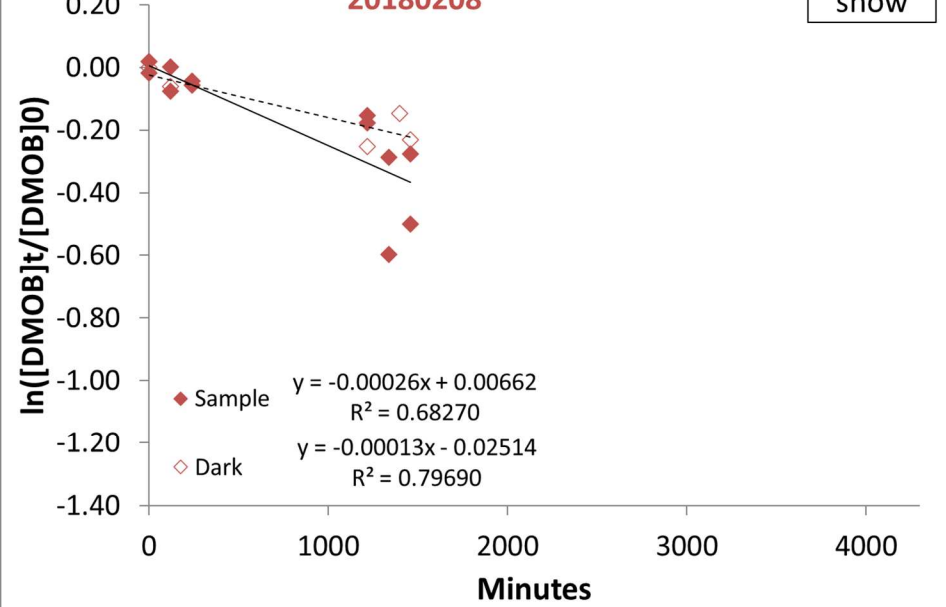
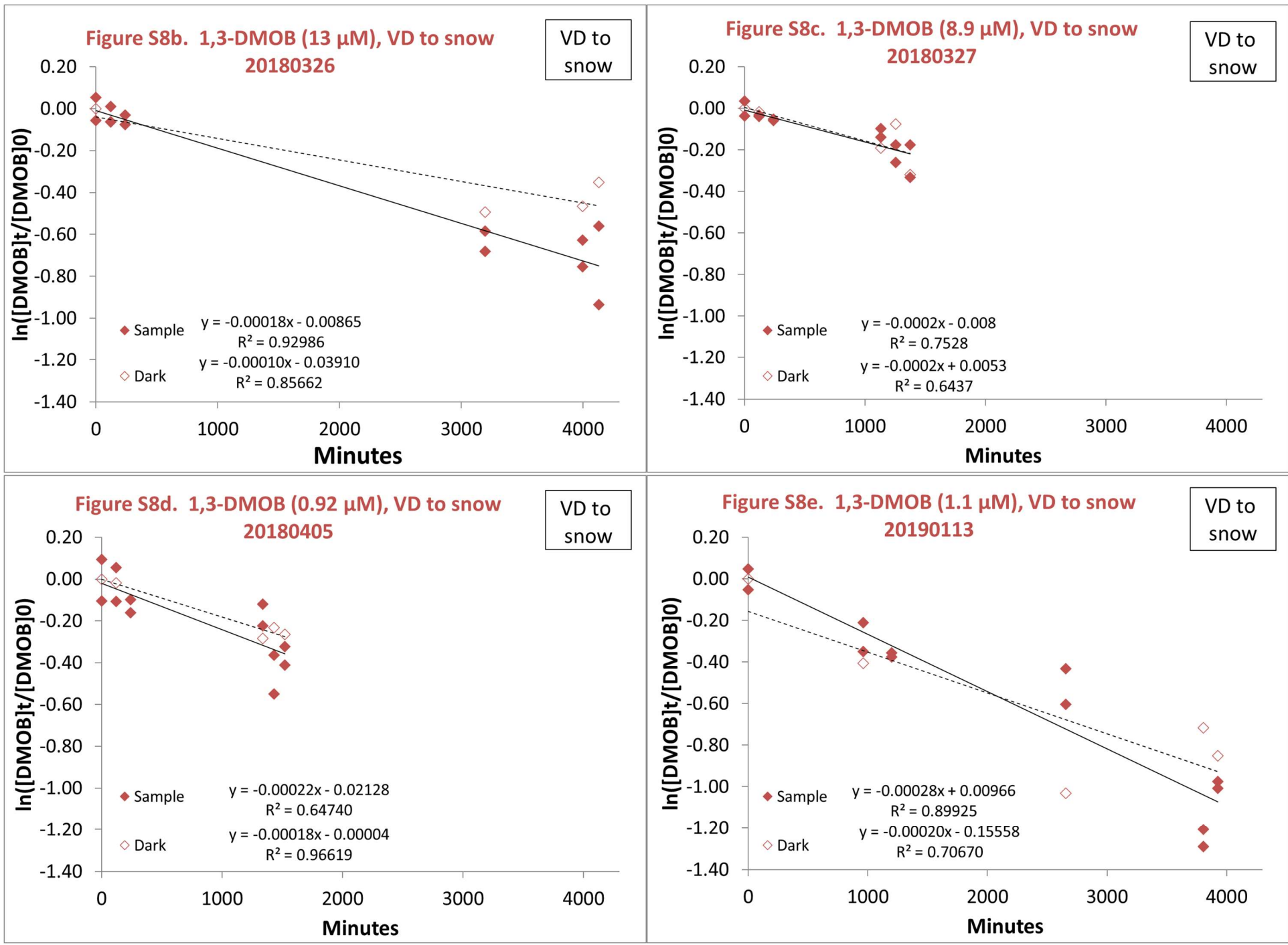


Figure S8a. 1,3-DMOB (1.0 μ M), VD to snow
20180208

VD to
snow





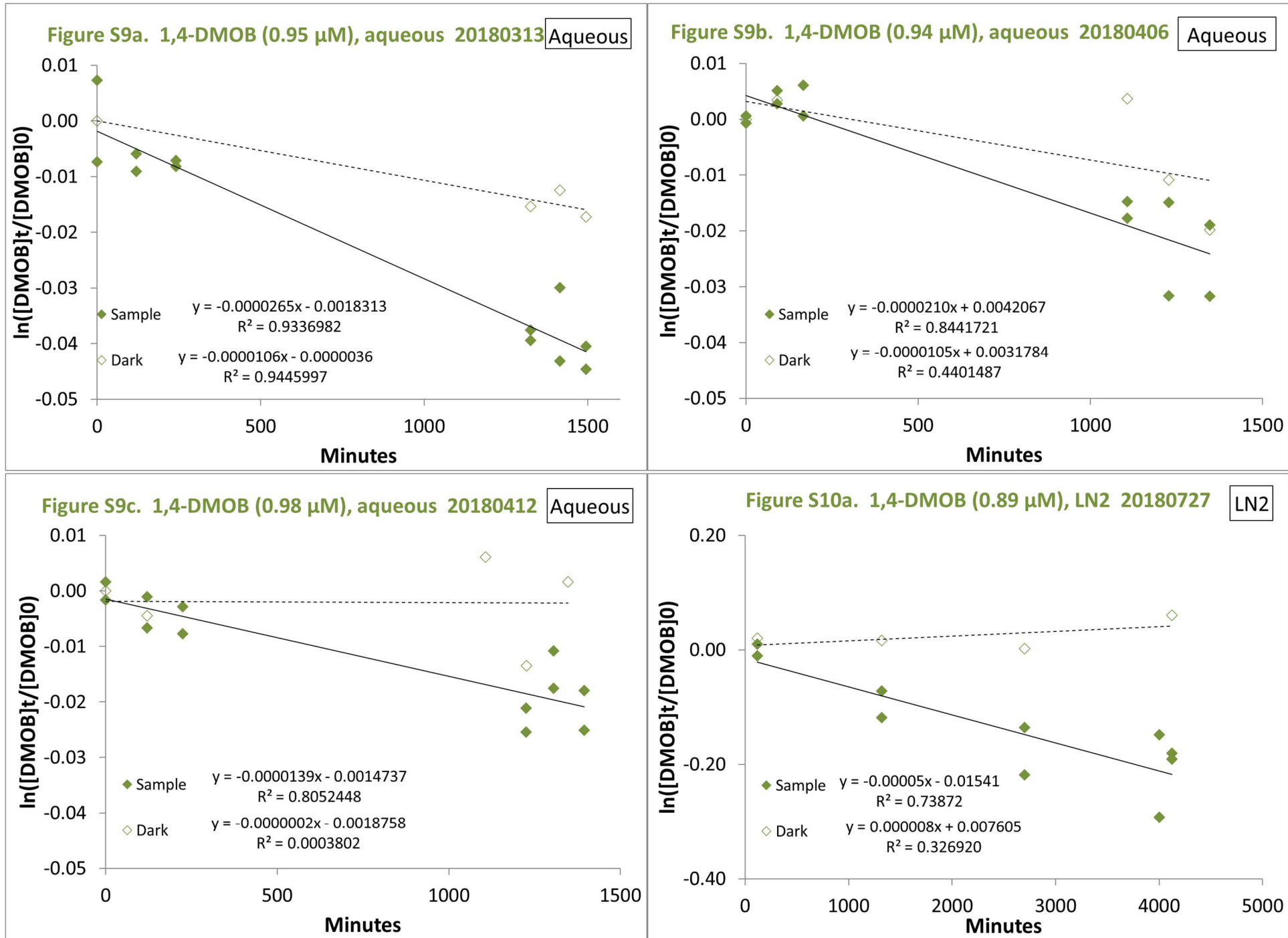


Figure S10b. 1,4-DMOB (1.1 μ M), LN2 20180802

LN2

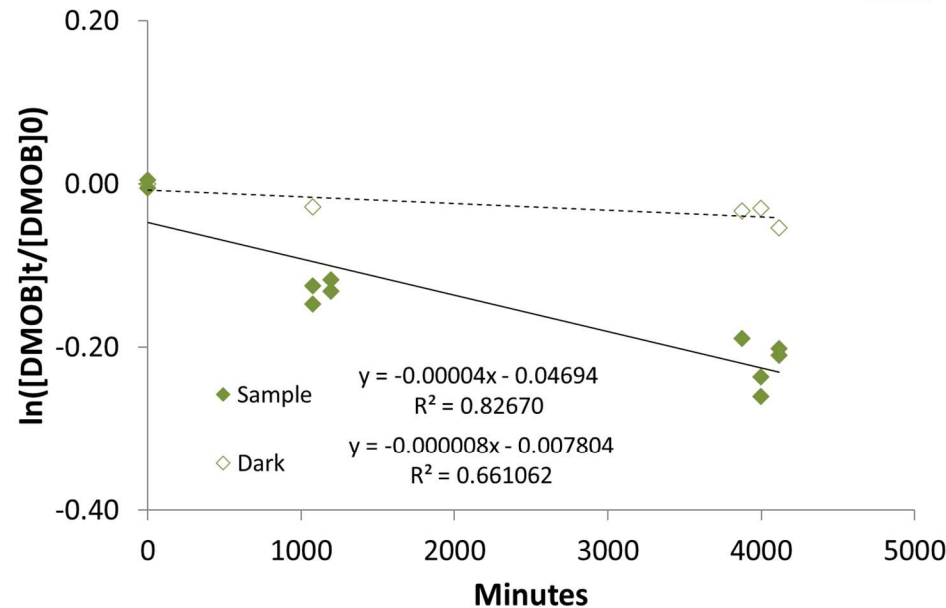


Figure S10c. 1,4-DMOB (0.91 μ M), LN2 20180910

LN2

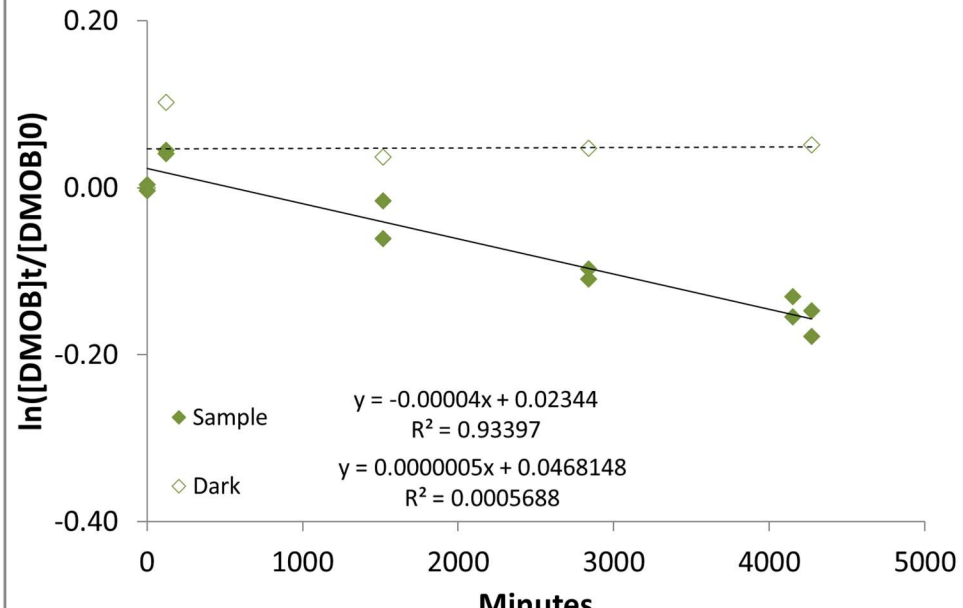


Figure S11a. 1,4-DMOB (9.5 μ M), VD to ice surface
20180712

VD to
ice surface

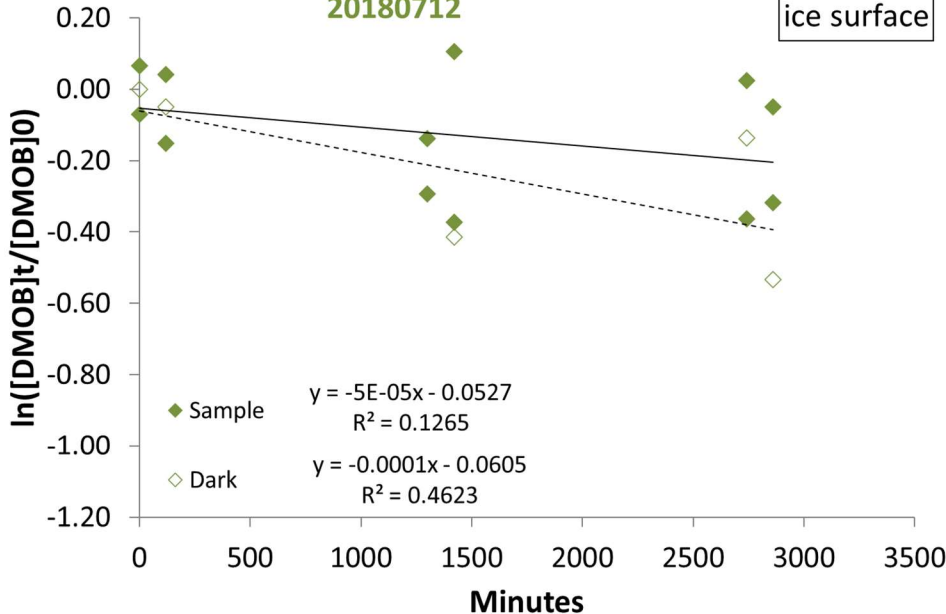
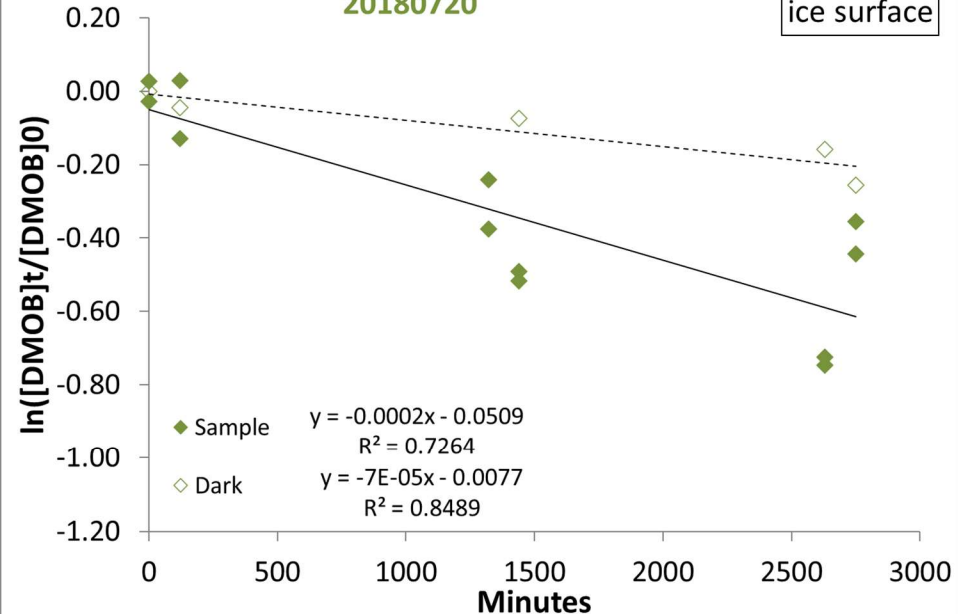
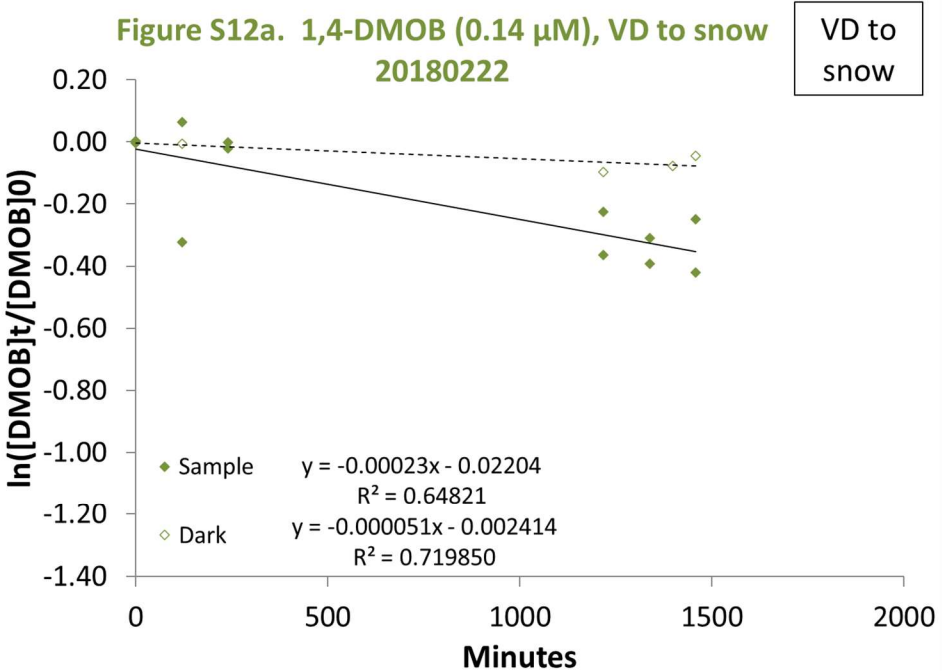
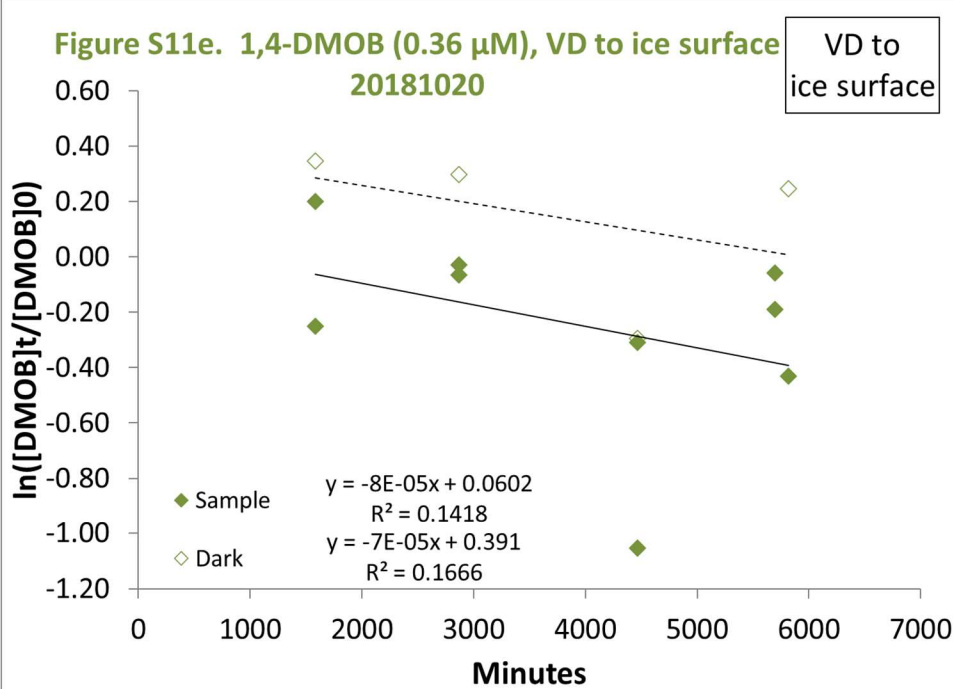
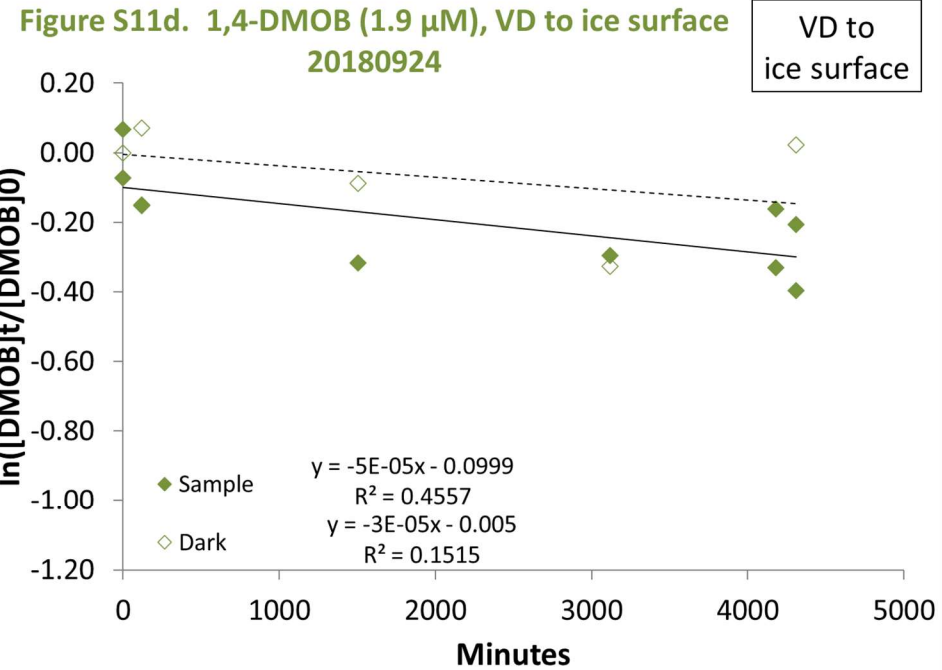
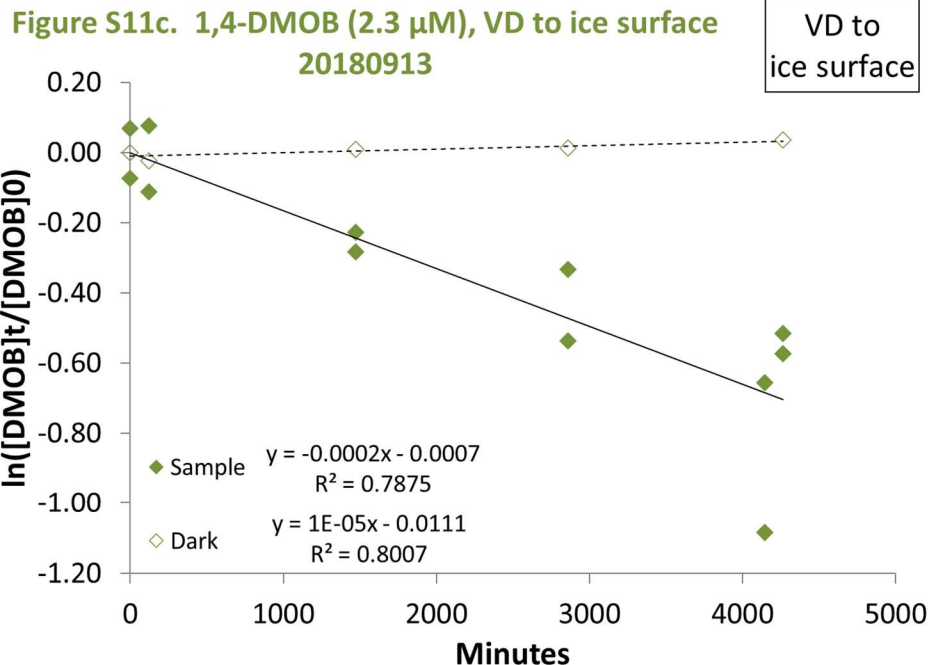
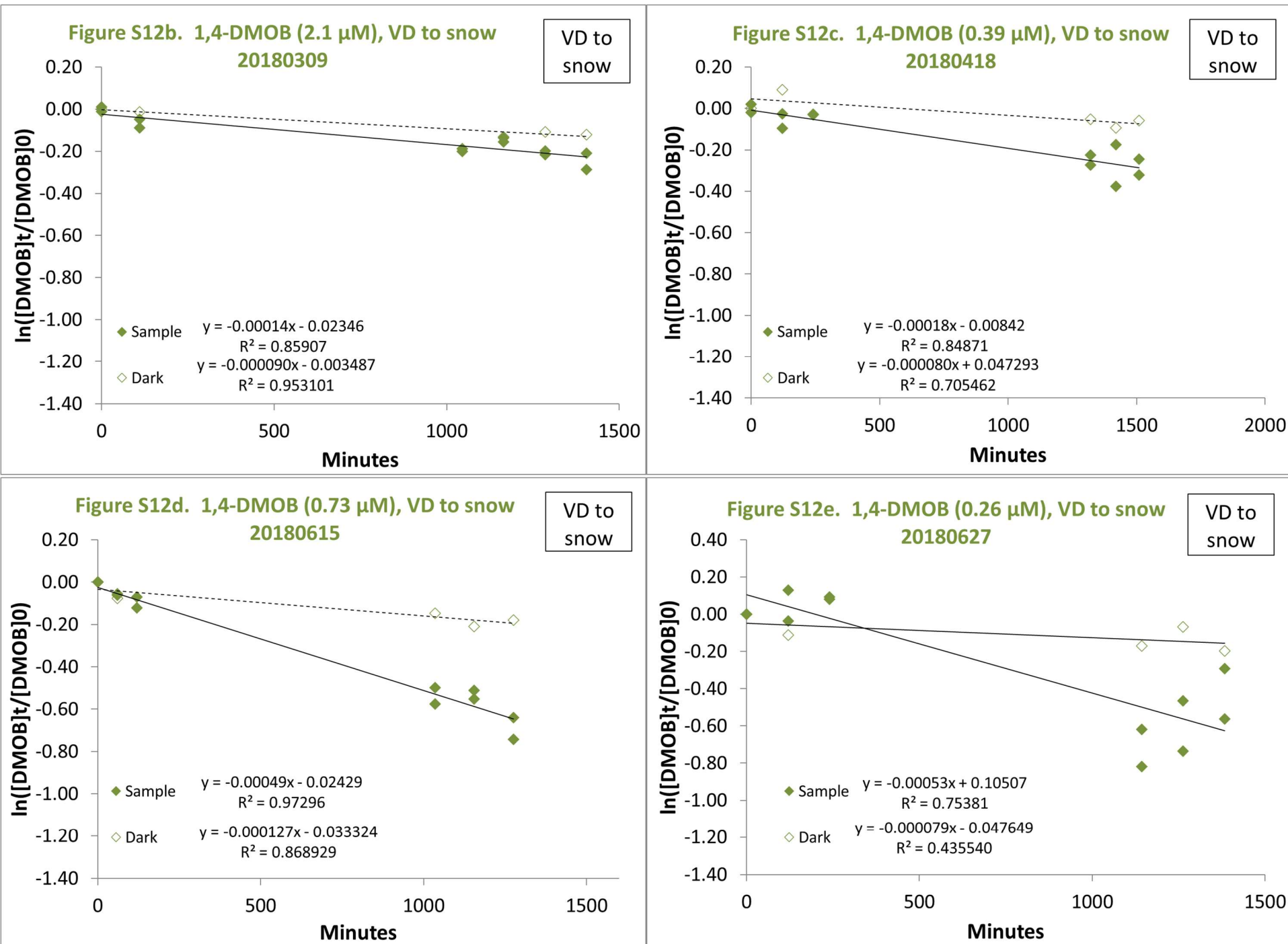


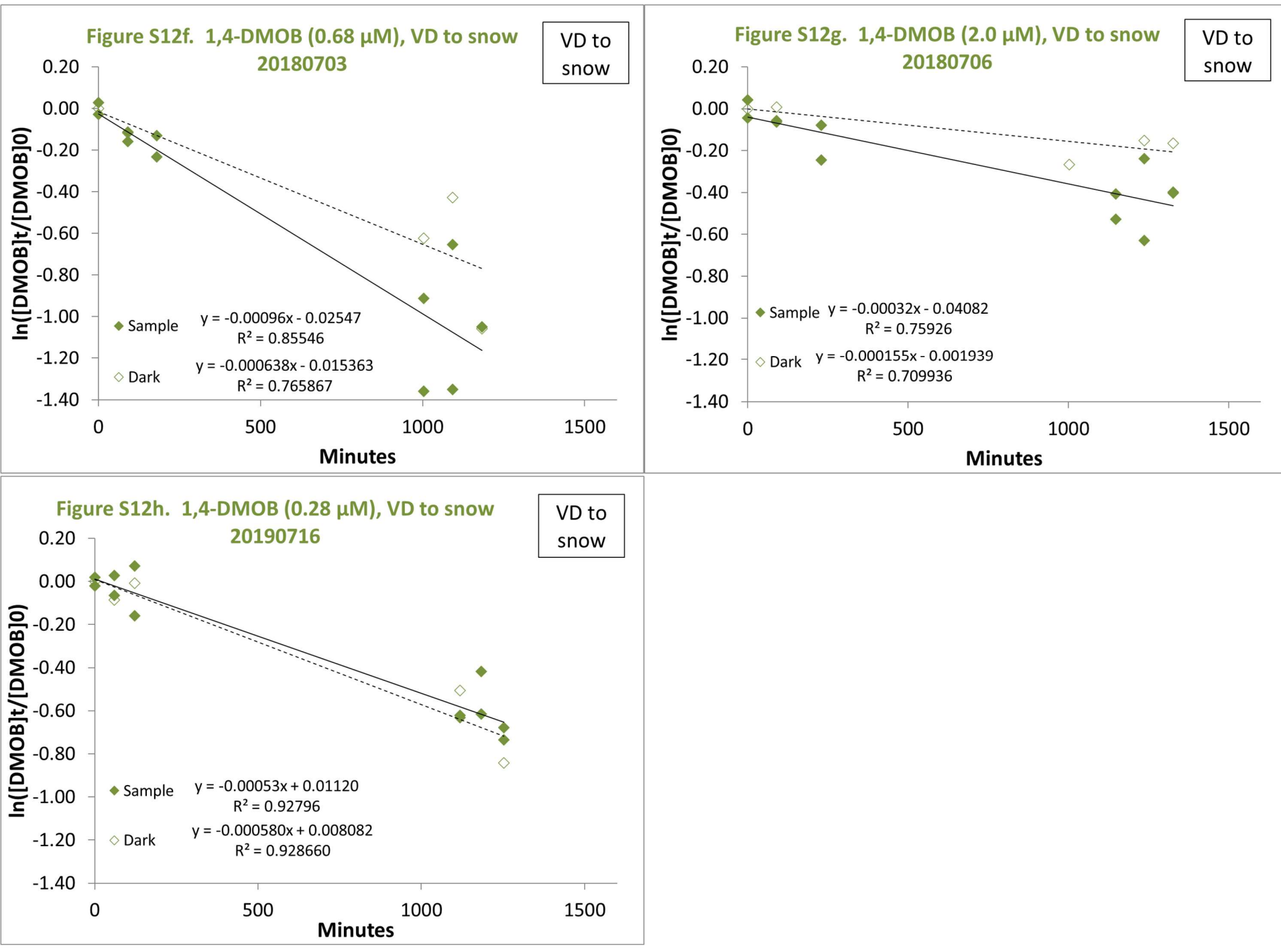
Figure S11b. 1,4-DMOB (3.0 μ M), VD to ice surface
20180720

VD to
ice surface

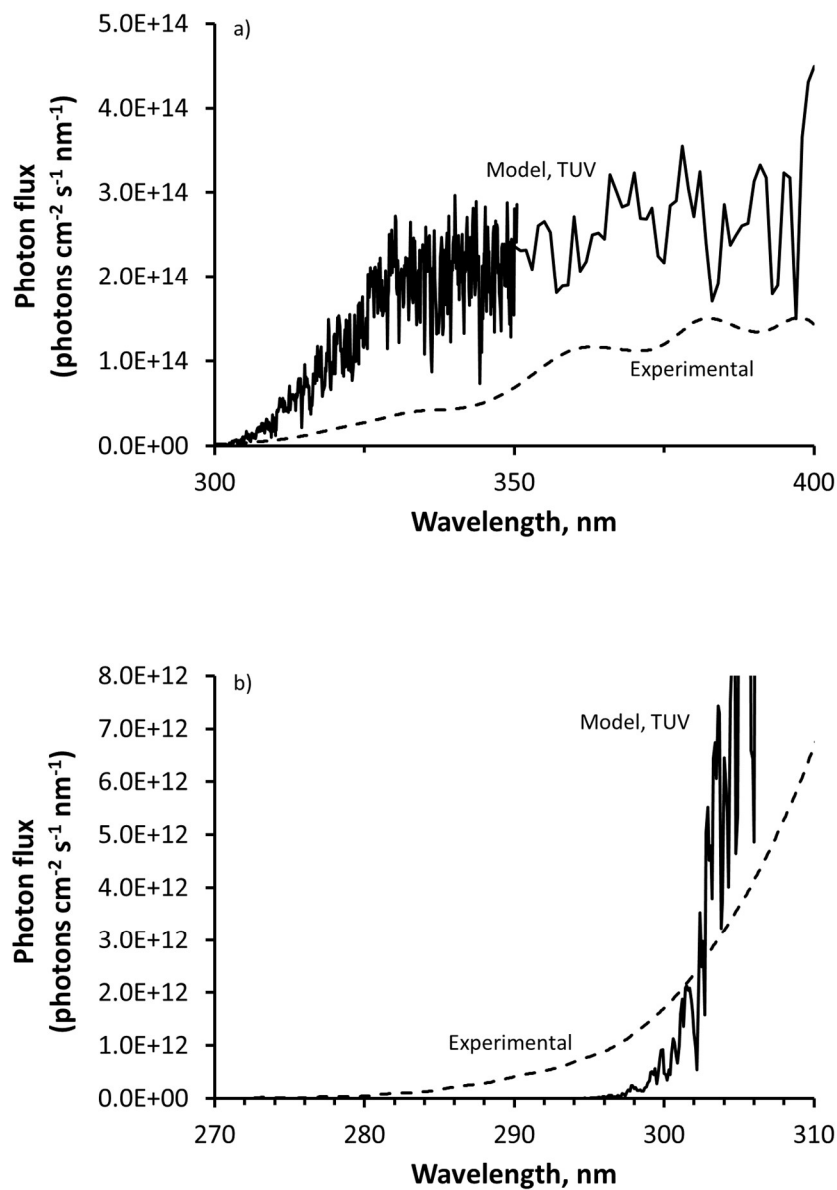




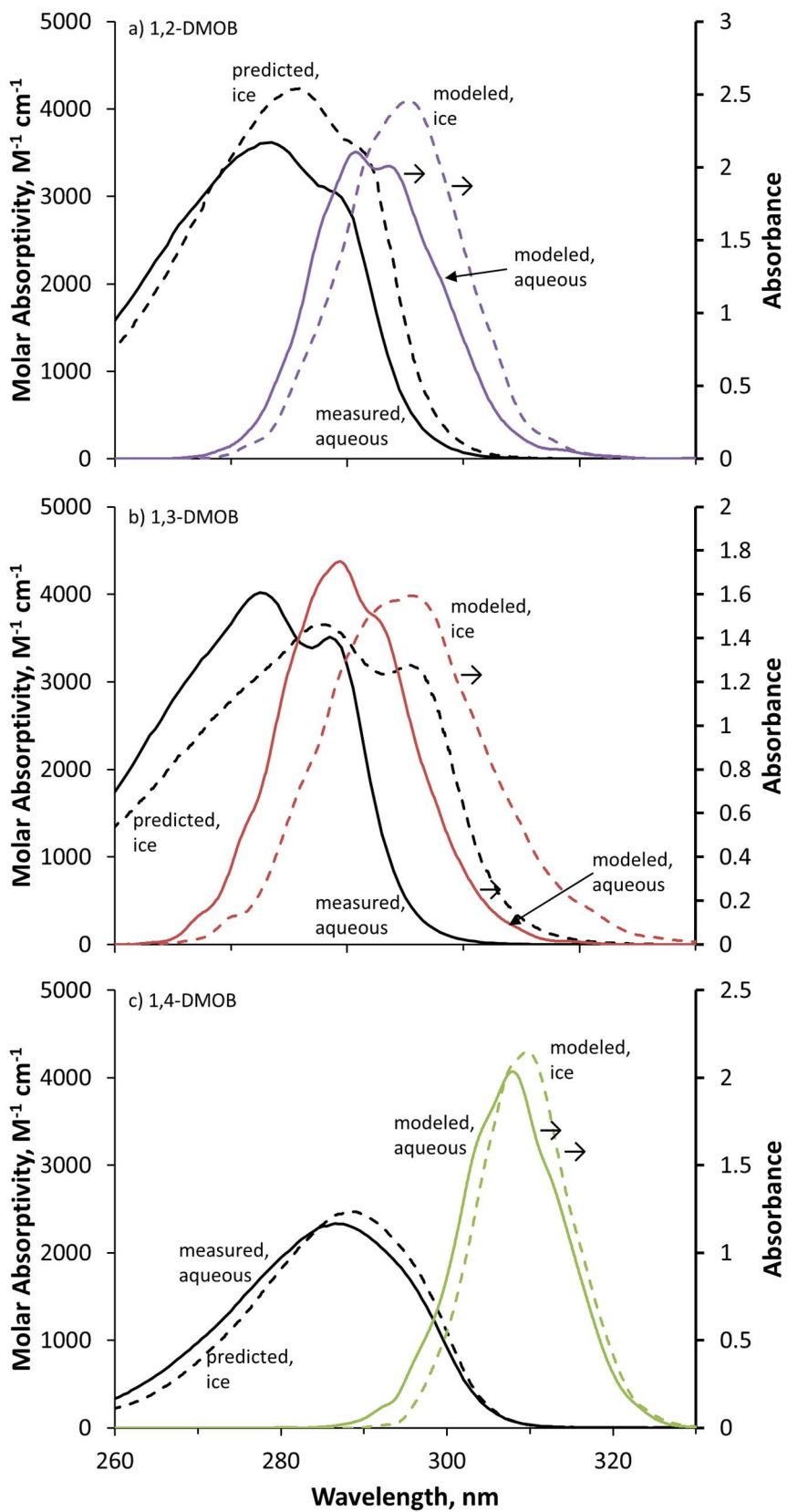




Supplemental Figures S1a-S12h. Results for individual illumination experiments. Results for individual illumination experiments showing dimethoxybenzene concentration changes over time for illuminated samples (filled diamonds, solid regression line) and dark controls (open diamonds, dashed regression line). Date for each experiment is given in yyyyymmdd format. Compounds are color-coded purple (1,2-DMOB), maroon (1,3-DMOB), and green (1,4-DMOB). Sample type is given in the upper right corner of each graph. Each data point represents an individual sample beaker, with two illuminated samples and one dark control sample per time point. Initial DMOB concentration, measured as average measured aqueous concentration in the two time zero illuminated samples, is given in the chart title. Wherever possible, for each compound the same Y axis scale was used for related sample treatments to allow easier comparison. Average data for each experiment type are summarized in Table S3.

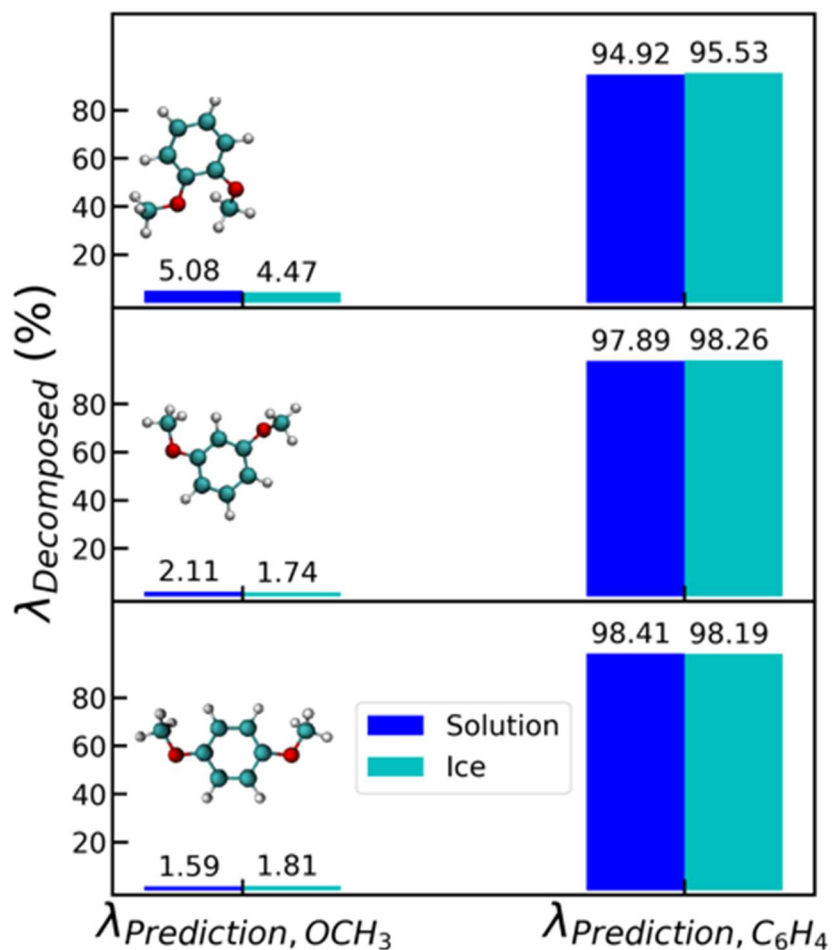


Supplemental Figure S13. Experimental and modeled photon fluxes. Experimental and TUV-modeled photon fluxes from 300-400 nm (panel a) and 270-310 nm (panel b). TUV-modeled flux is for Summit, Greenland at noon on the summer solstice (see text for details of modeling parameters). a) Summit actinic flux is given at 0.1 nm resolution from 300-350 nm, then 1 nm resolution from 350-400 nm; experimental flux was determined at 1 nm and interpolated to 0.1 nm resolution presented here. b) TUV and experimental fluxes at 0.1 nm resolution.

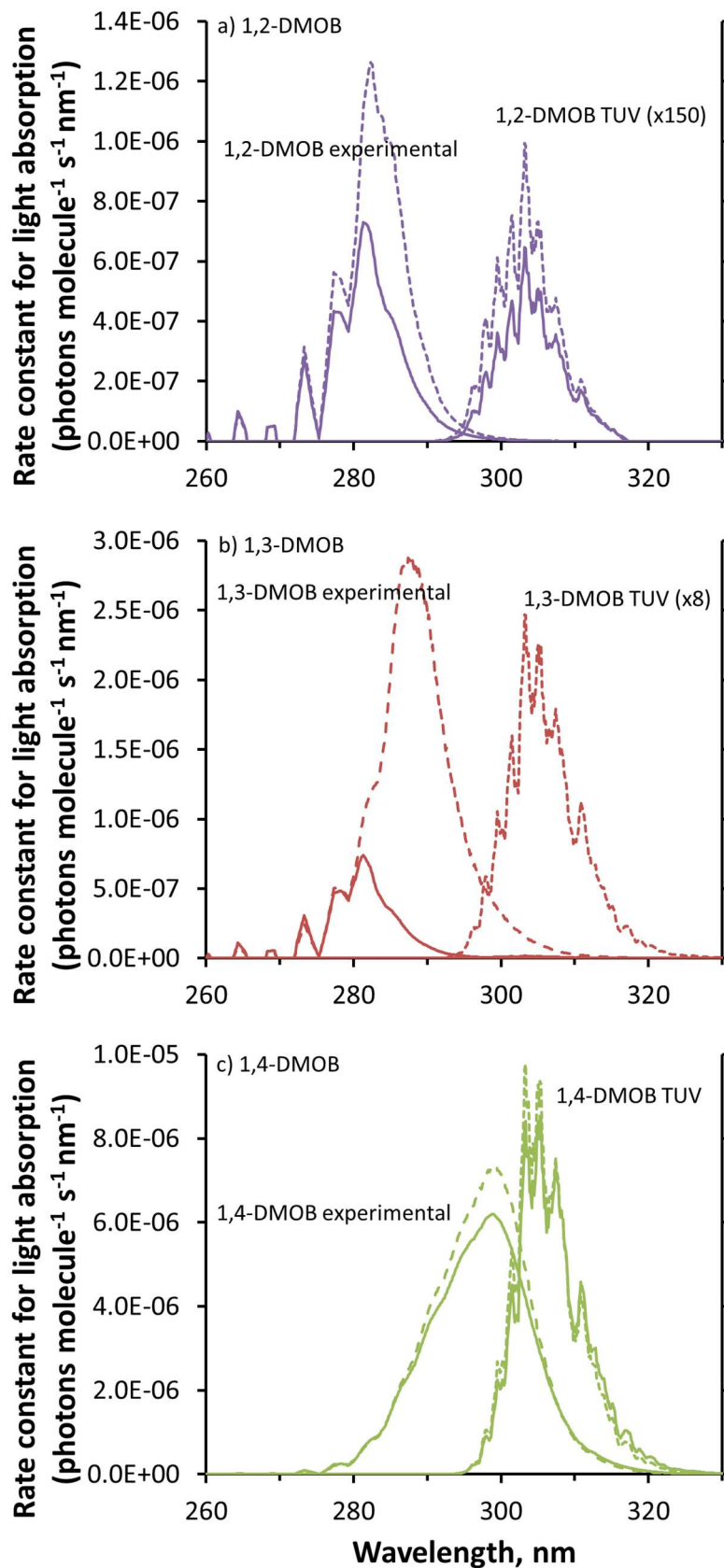


Supplemental Figure S14. Light absorbance spectra for DMOB isomers. Measured and modeled spectra for 1,2-, 1,3-, and 1,4-DMOB. For each isomer, solid black lines are the measured absorbance spectra in aqueous solution; solid and dashed colored lines are the aqueous and air-ice interface spectra estimated using molecular modeling (right axis); dashed black lines show the air-ice interface absorbance values predicted by combining

the measured aqueous absorbance spectra with the modeling results (see text for details). Modeled absorbance values (right axis) are arbitrary and not intended to correspond to actual molar absorption coefficients.



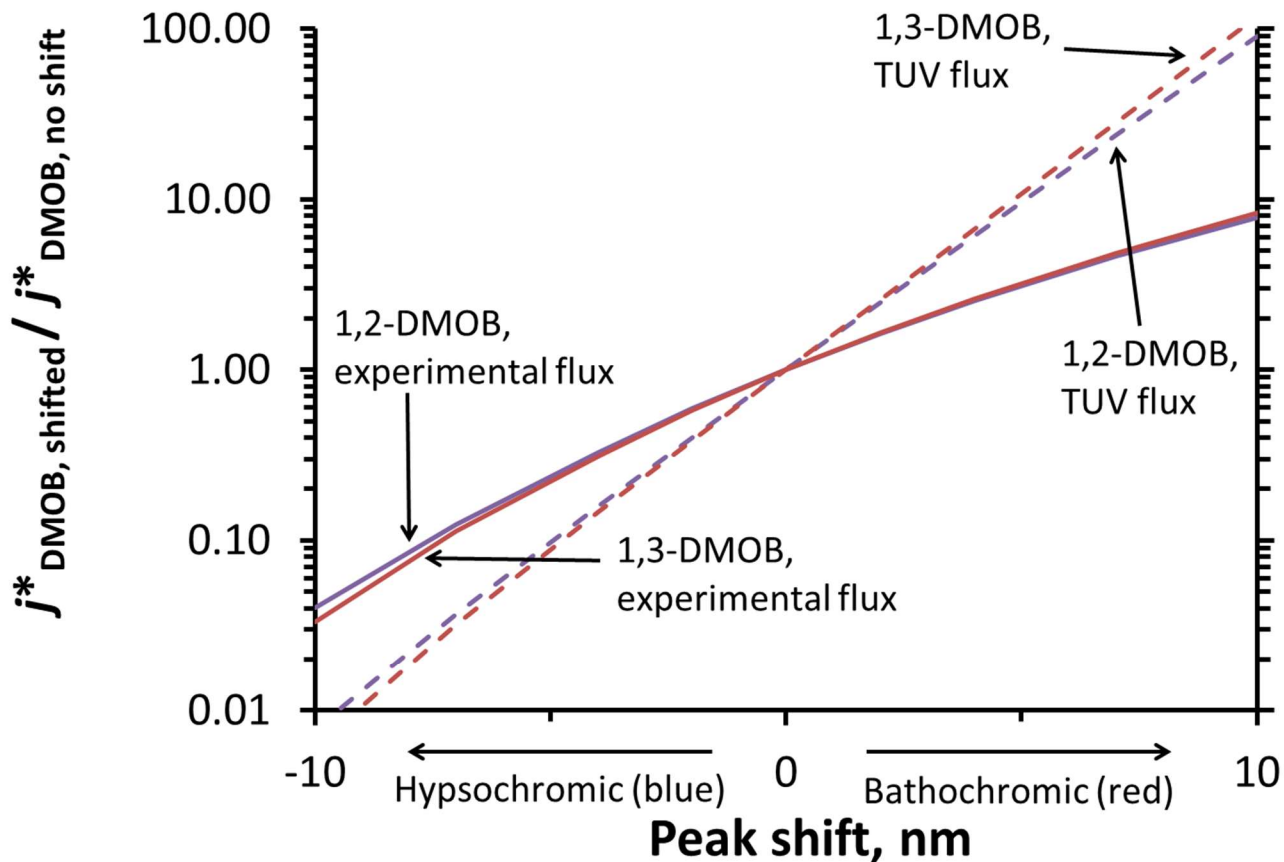
Supplemental Figure S15. Linear decomposition analysis for DMOB isomers. Linear Decomposition Analysis for the $\lambda_{predictions}$ for the three DMOB isomers. Bars and values represent the contributions of the phenyl ring (C_6H_4) and methoxy group (OCH_3) to the predicted excitation wavelength ($\lambda_{Decomposed}$) for 1,2- (top), 1,3- (middle) and 1,4-DMOB (bottom) in solution (blue) and at the air-ice interface (cyan).



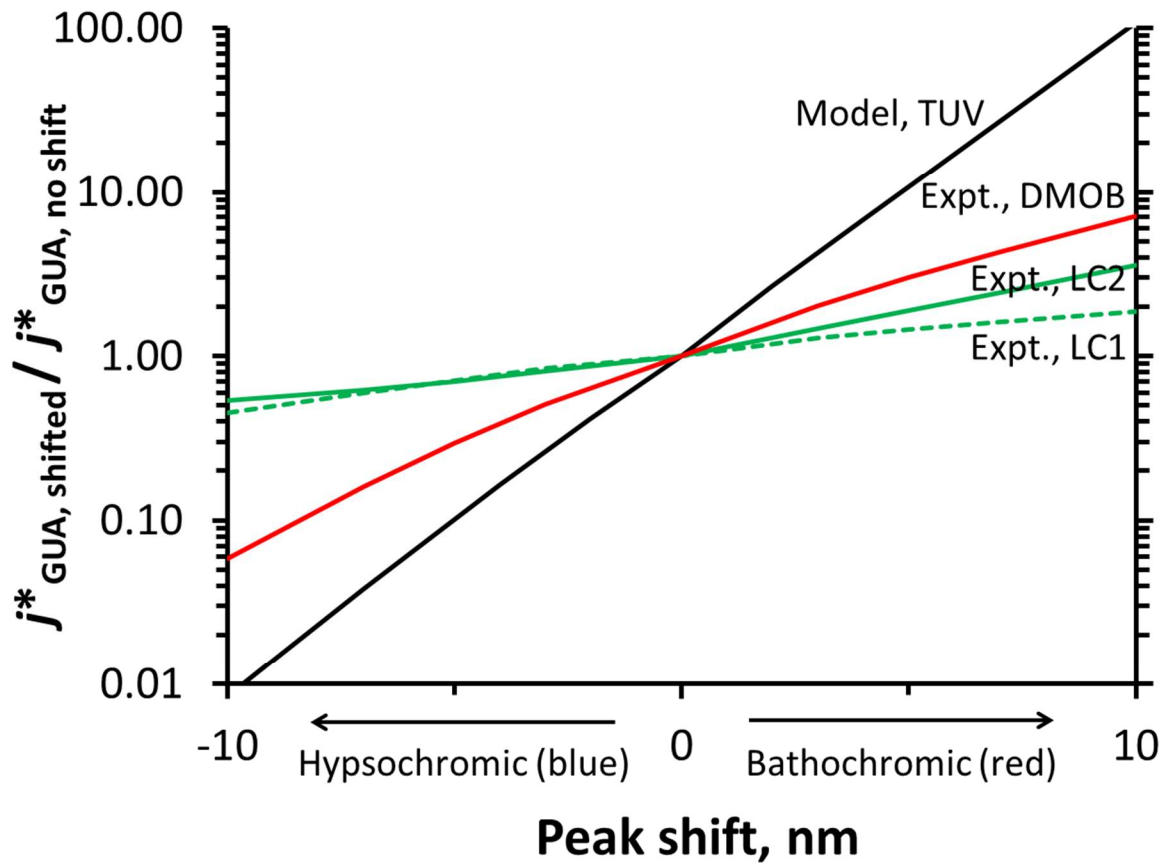
Supplemental Figure S16. Action spectra for DMOB light absorbance. Action spectra for light absorbance, determined for each DMOB isomer by multiplying the aqueous (solid lines) or predicted air-ice interface (dashed lines) molar absorption coefficient by the experimental or Summit conditions photon flux at each wavelength. Results are given at 1 nm resolution. The value at a given wavelength was determined as

$$\frac{2303}{N_A} I_\lambda \varepsilon_\lambda$$

where 2303 is a factor for units and base conversion ($1000 \text{ cm}^3 \text{ L}^{-1}$), N_A is Avogadro's number ($6.022 \times 10^{23} \text{ molecules mol}^{-1}$), I_λ is the photon flux at each wavelength ($\text{photons cm}^{-2} \text{ s}^{-1}$), and ε_λ is the wavelength-dependent molar absorption coefficient for each DMOB ($\text{M}^{-1} \text{ cm}^{-1}$). The area under each curve is the overall rate constant for light absorbance; these are tabulated in Table S4. For 1,2- and 1,3-DMOB, the Summit conditions rate constants have been scaled for readability.

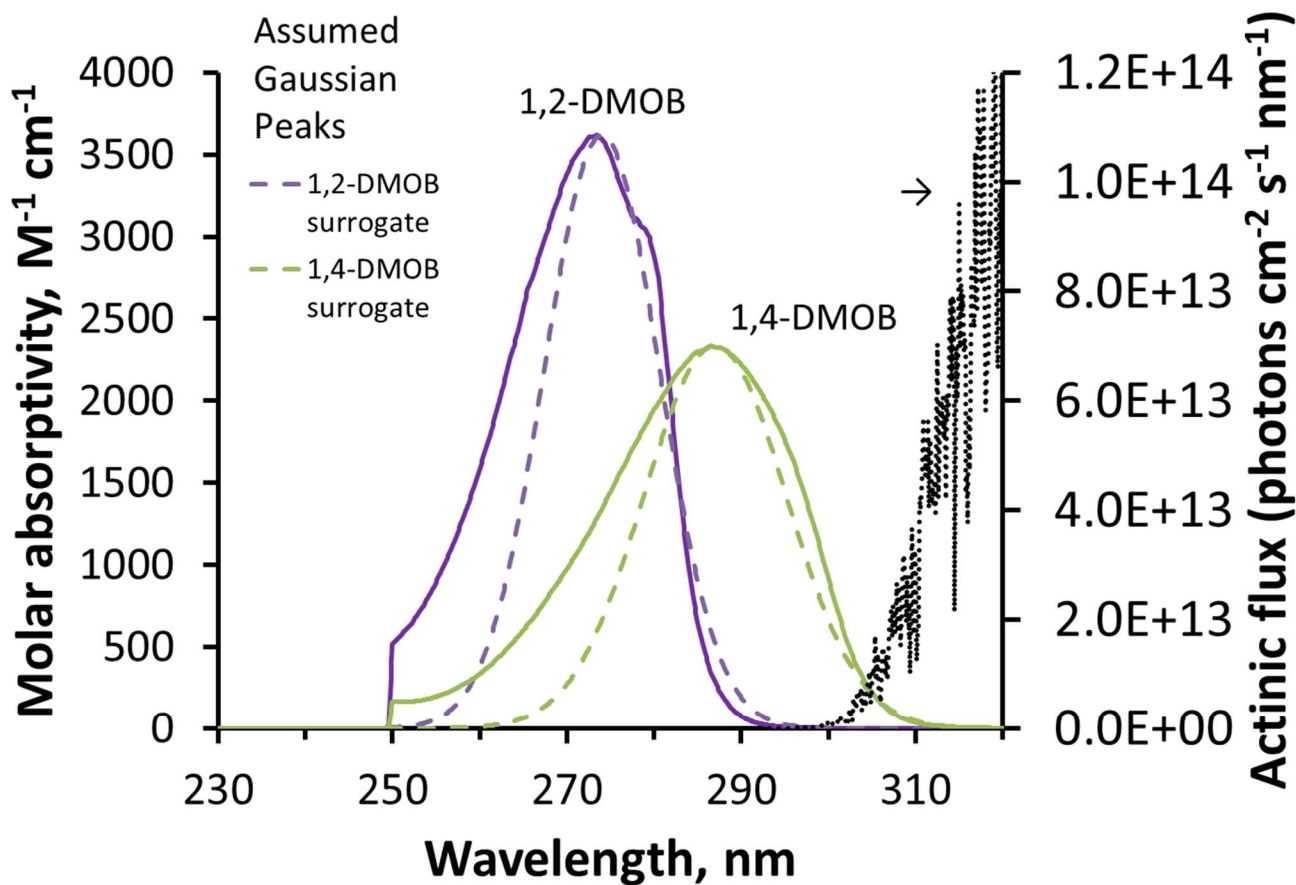


Supplemental Figure S17. Photodegradation rate constant ratios for shifted absorbance curves. Predicted changes in photodegradation rate constants (j^*_{DMOB}) for 1,2- and 1,3-DMOB due to shifting of absorbance relative to the unshifted value where the peak is centered at 280 nm. Rate constants were estimated using calculated quantum yields, aqueous absorbance spectra shifted hypsochromically (towards shorter wavelengths) or bathochromically (towards longer wavelengths), and either experimental photon fluxes (solid lines) or the TUV-modeled actinic flux for midday on the summer solstice at Summit, Greenland (dashed lines). See Figure 4 for the equivalent figure for 1,2- and 1,4-DMOB.

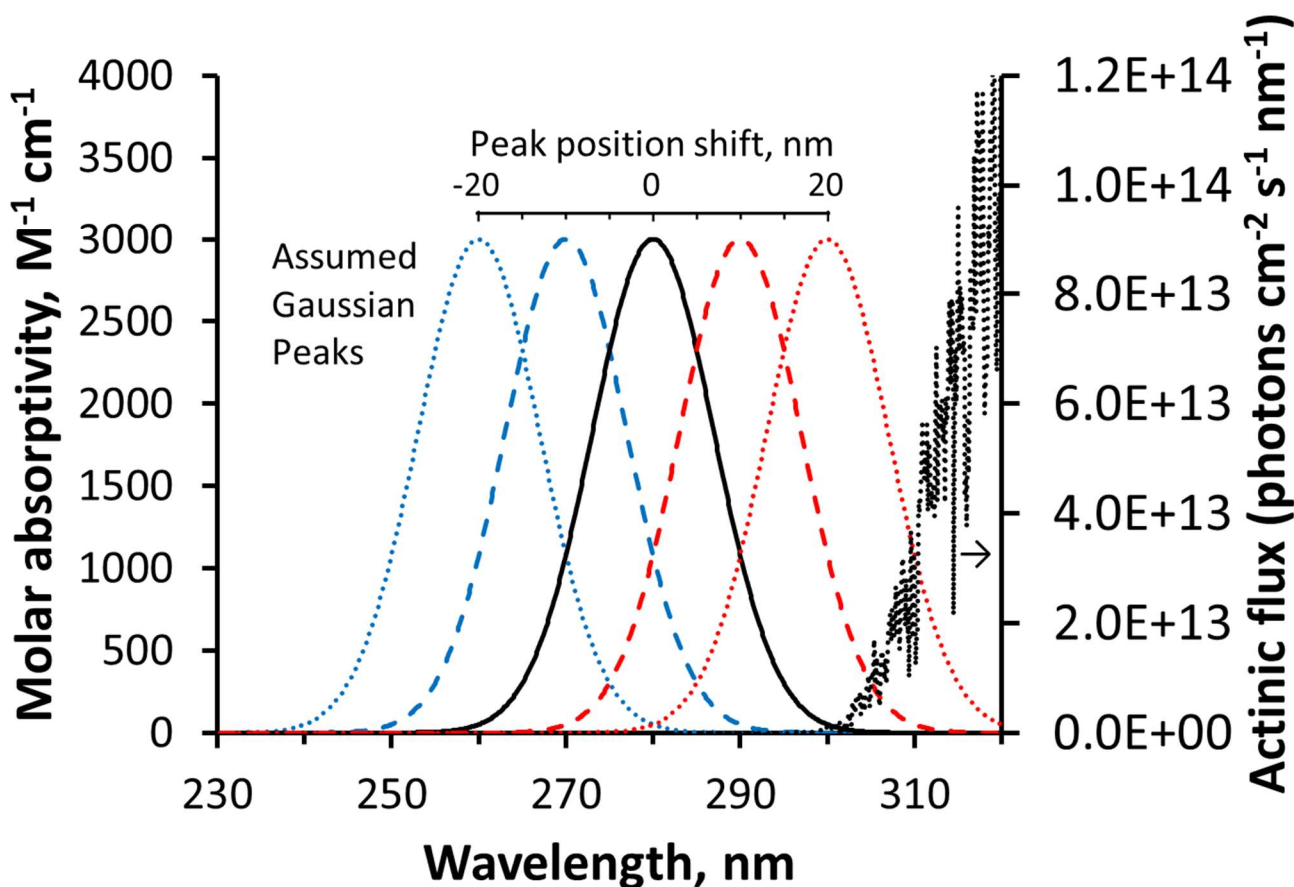


Supplemental Figure S18. Guaiacol photodegradation rate constants for various illumination conditions.

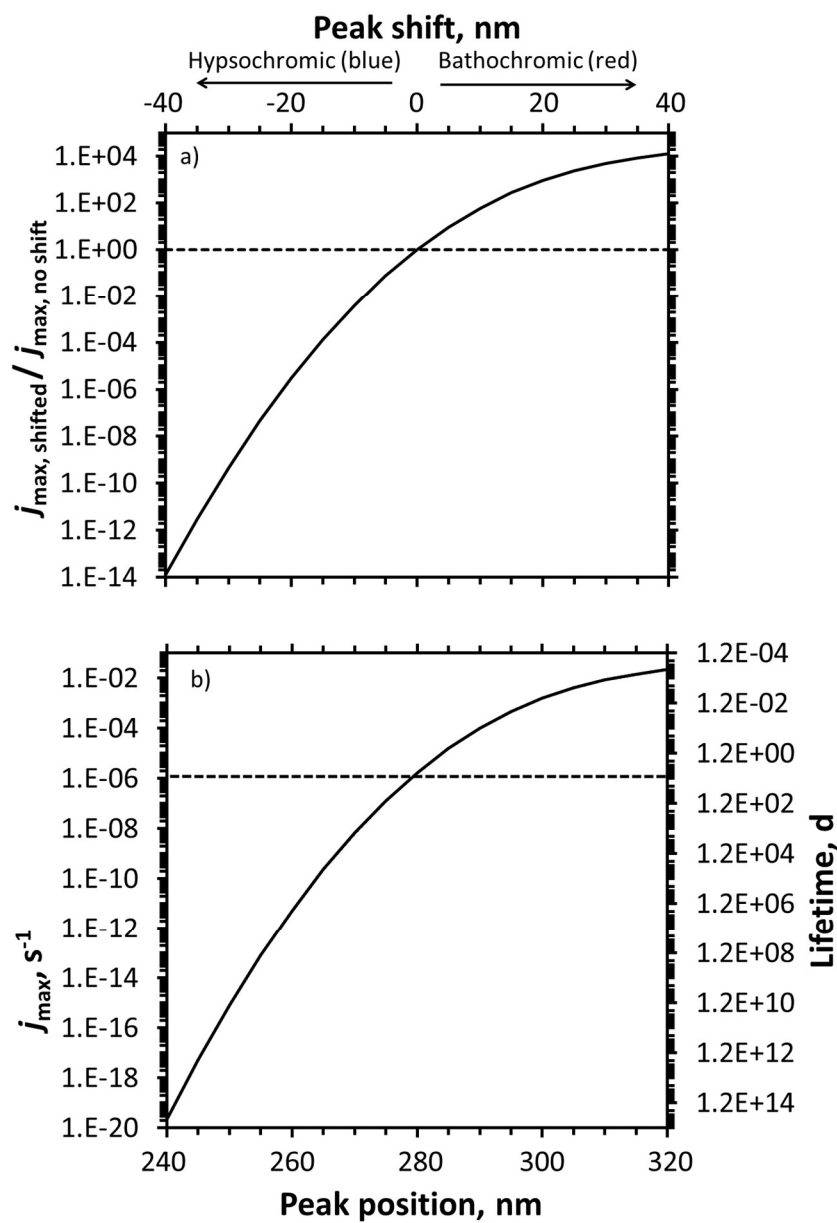
Absorbance shift impacts on calculated guaiacol photodegradation rate constants under several photon flux conditions. The black line represents rate constants calculated using TUV-modeled photon fluxes for Summit, Greenland at noon on the summer solstice; the red line uses the photon fluxes for experiments in this work; the green lines were calculated using the two experimental light conditions used in our previous guaiacol work (Hullar et al. 2020). The difference in photon fluxes between the solid red (DMOB) and green (LC2) lines is due to changing the cover material for the sample beaker: the current DMOB work uses a nylon film, while the previous LC2 guaiacol work used a polyethylene film.



Supplemental Figure S19. Absorbance spectra for DMOBs compared to assumed Gaussian peaks. Measured absorbance spectra and assumed Gaussian peaks for 1,2- and 1,4-dimethoxybenzene. Solid lines are the measured aqueous absorbance spectra, and the dashed lines are the Gaussian distributions chosen to approximate the measured spectra. The 1,2-DMOB and 1,4-DMOB surrogates have peak locations, standard deviations, and peak heights of 274 and 287 nm, 6.6 and 8.3 nm, and 368 and $2335 \text{ M}^{-1} \text{ cm}^{-1}$ respectively. Black dashed line (right axis) represents the TUV-modeled actinic flux for Summit, Greenland.

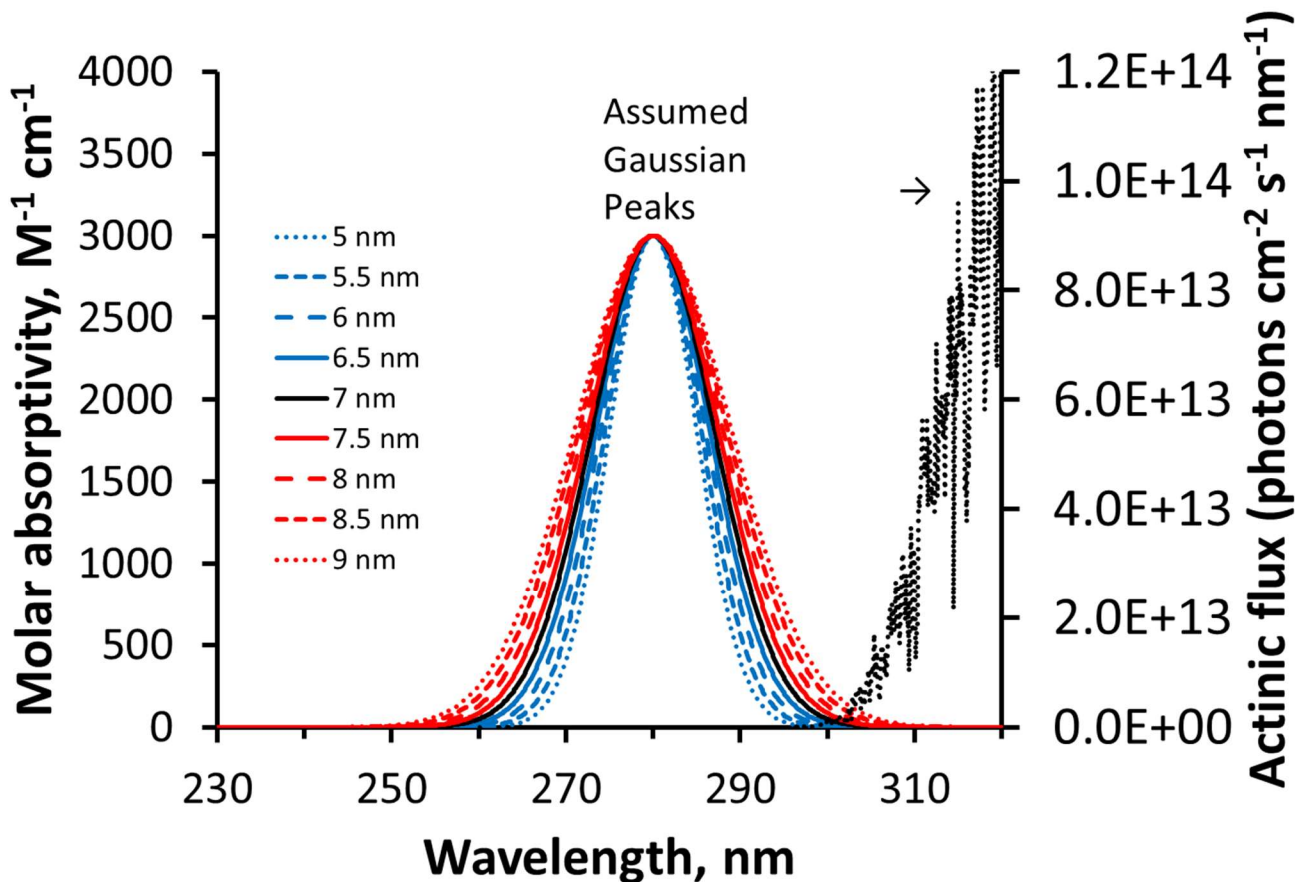


Supplemental Figure S20. Model compound absorbance spectra for various peak locations. Hypothetical model compound peak location with various position shifts. The solid black line represents the default center position of the assumed Gaussian peak (280 nm, standard deviation 7 nm, peak height $3000 \text{ M}^{-1} \text{ cm}^{-1}$), while blue and red lines show hypsochromically and bathochromically shifted peak locations, respectively. The black dashed line (right axis) represents the TUV-modeled actinic flux for Summit, Greenland.

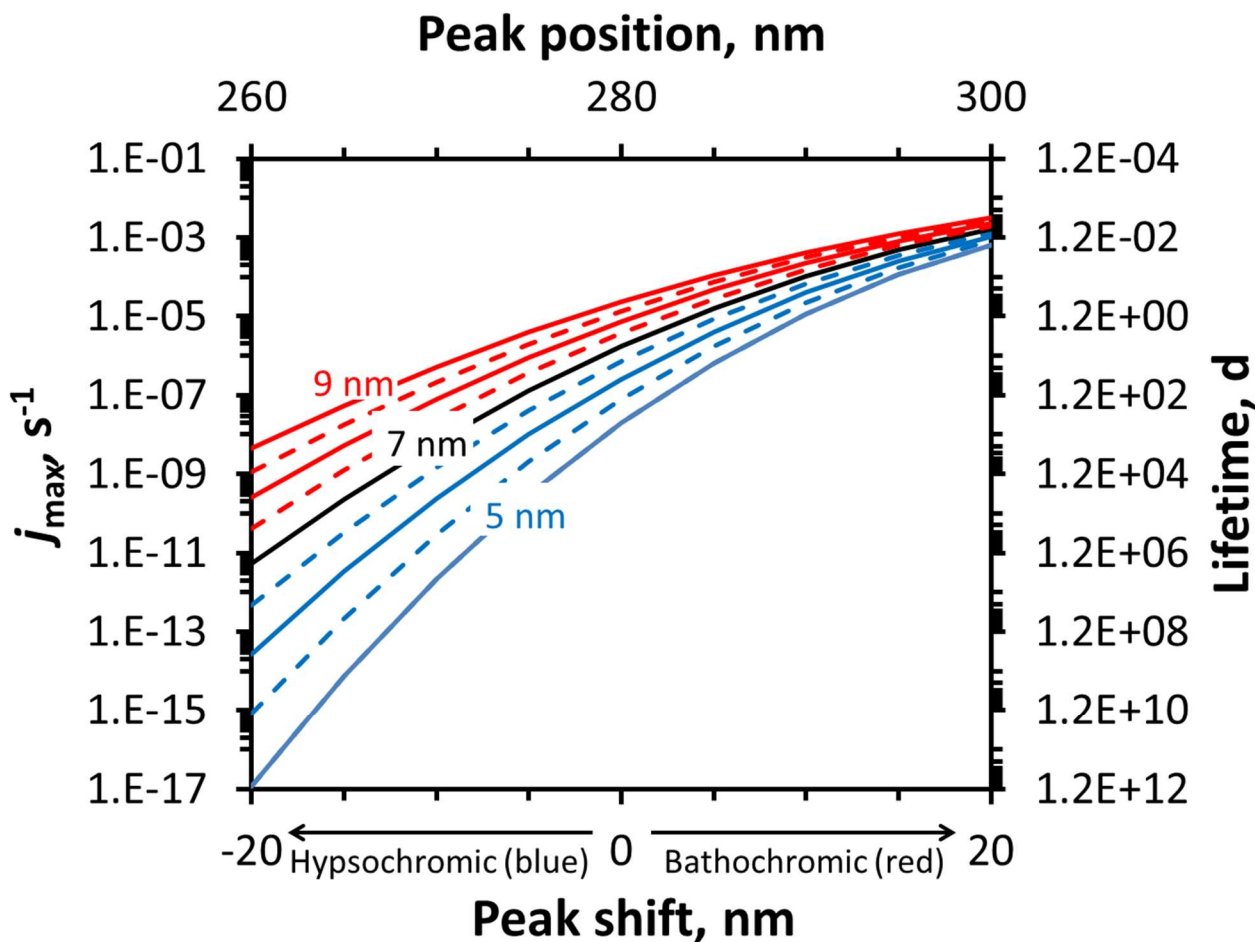


Supplemental Figure S21. Model compound photodegradation rate constants for various peak locations.

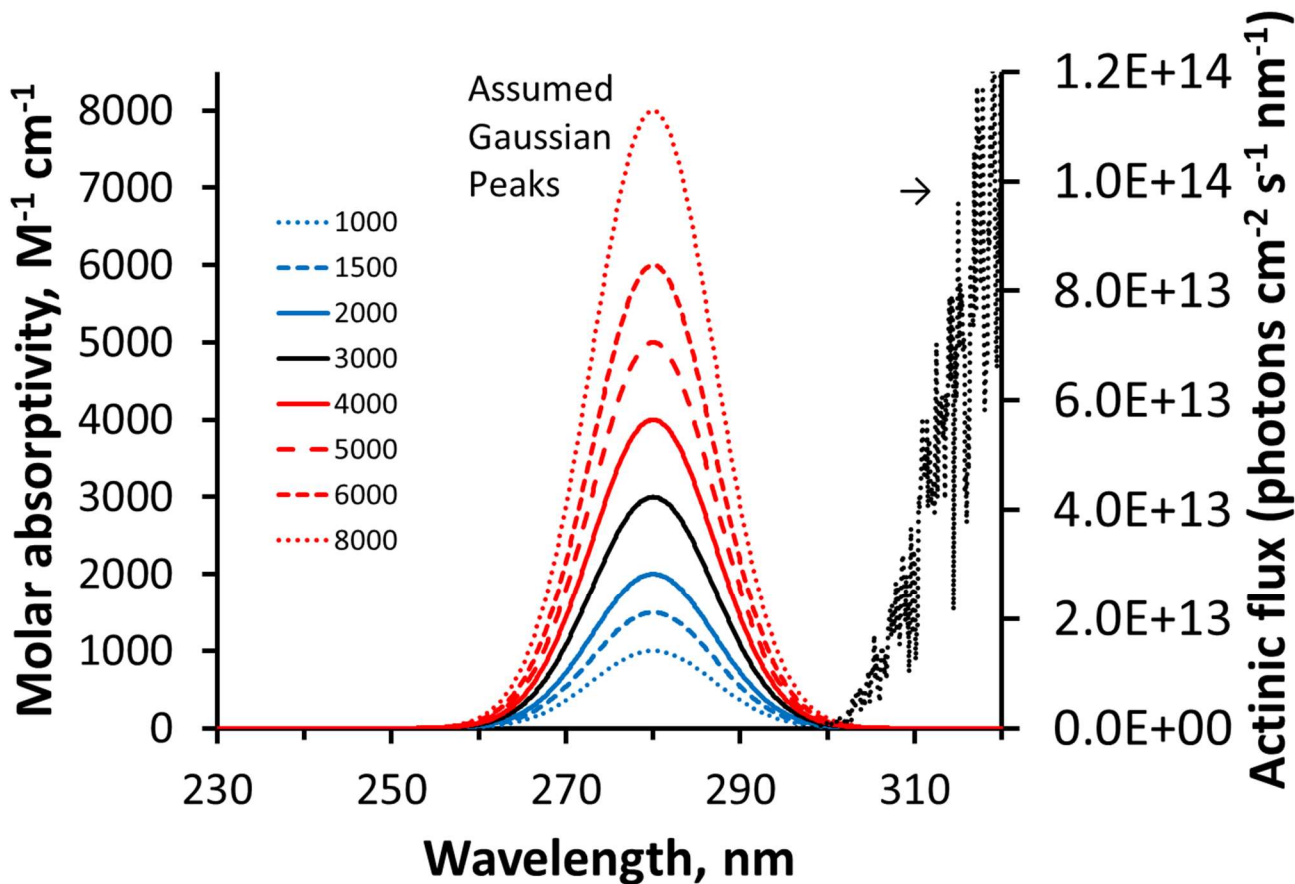
Predicted changes to photodegradation rate constants (j_{\max}) and the corresponding lifetimes resulting from absorbance shifts for a hypothetical model compound. Rate constants (j_{\max}) and lifetimes were calculated using an assumed quantum yield of 1, modeled actinic flux for Summit conditions, and an assumed Gaussian absorbance spectrum (peak molar absorption coefficient $3000 \text{ M}^{-1} \text{ cm}^{-1}$, standard deviation of 7 nm) with varying peak positions. a) Ratio of shifted to unshifted j_{\max} for varying hypsochromic (blue) or bathochromic (red) absorbance shifts. b) Calculated rate constants (j_{\max}) and lifetimes at various peak positions.



Supplemental Figure S22. Model compound absorbance spectra for various peak widths. Assumed absorption spectrum for a Gaussian hypothetical model compound showing baseline peak width (black line, standard deviation 7 nm) and various other peak widths (red and blue lines). Black dashed line (right axis) represents the TUV-modeled actinic flux for Summit, Greenland.

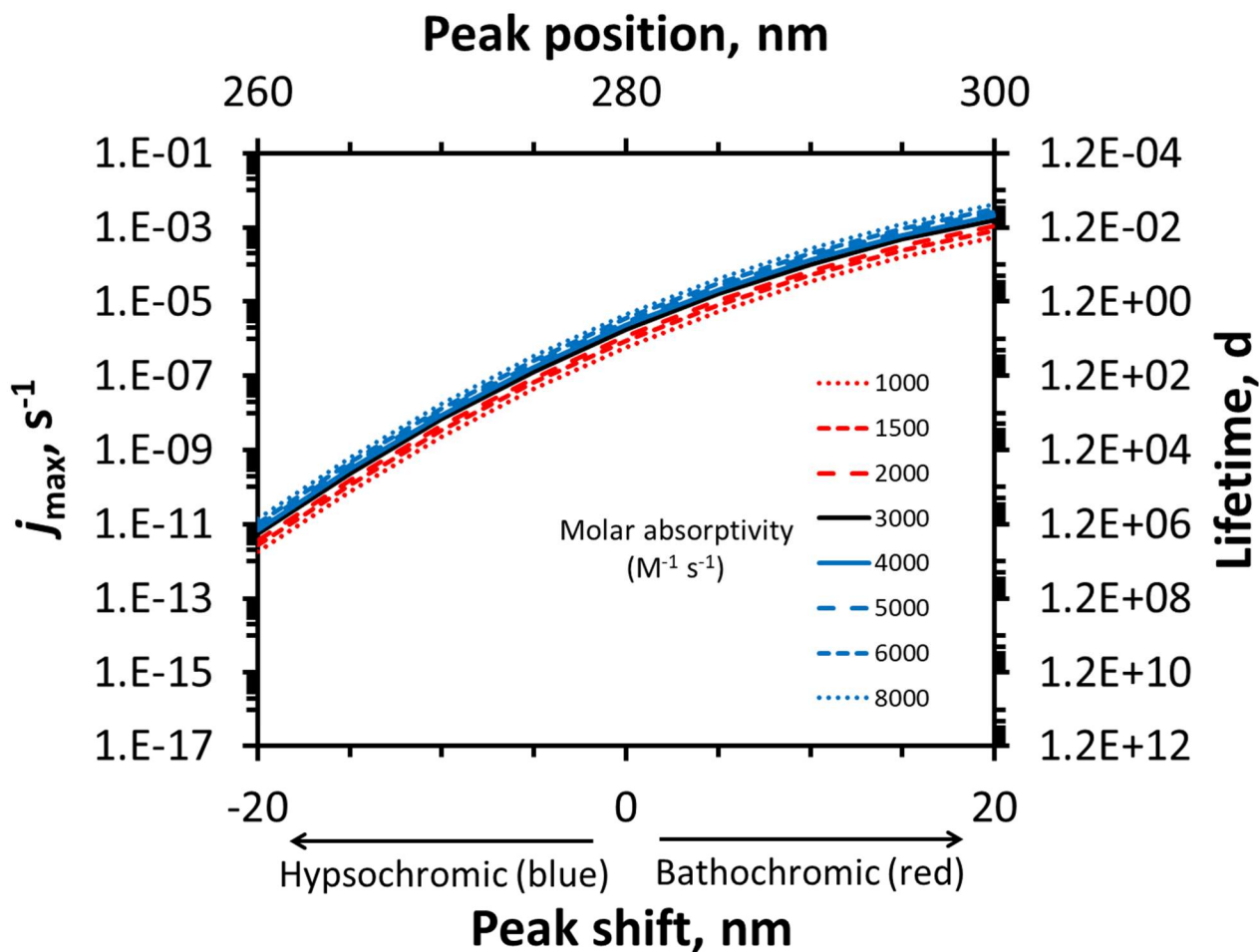


Supplemental Figure S23. Model compound photodegradation rate constants for various peak widths.
 Predicted changes to photodegradation rate constants and photochemical lifetimes resulting from variations in peak width (represented by various standard deviations of an assumed Gaussian absorbance spectrum) for a hypothetical model compound. The solid black line shows the baseline peak width (7 nm), while the red and blue lines show the rate constants and lifetimes for various peak widths and shifts.

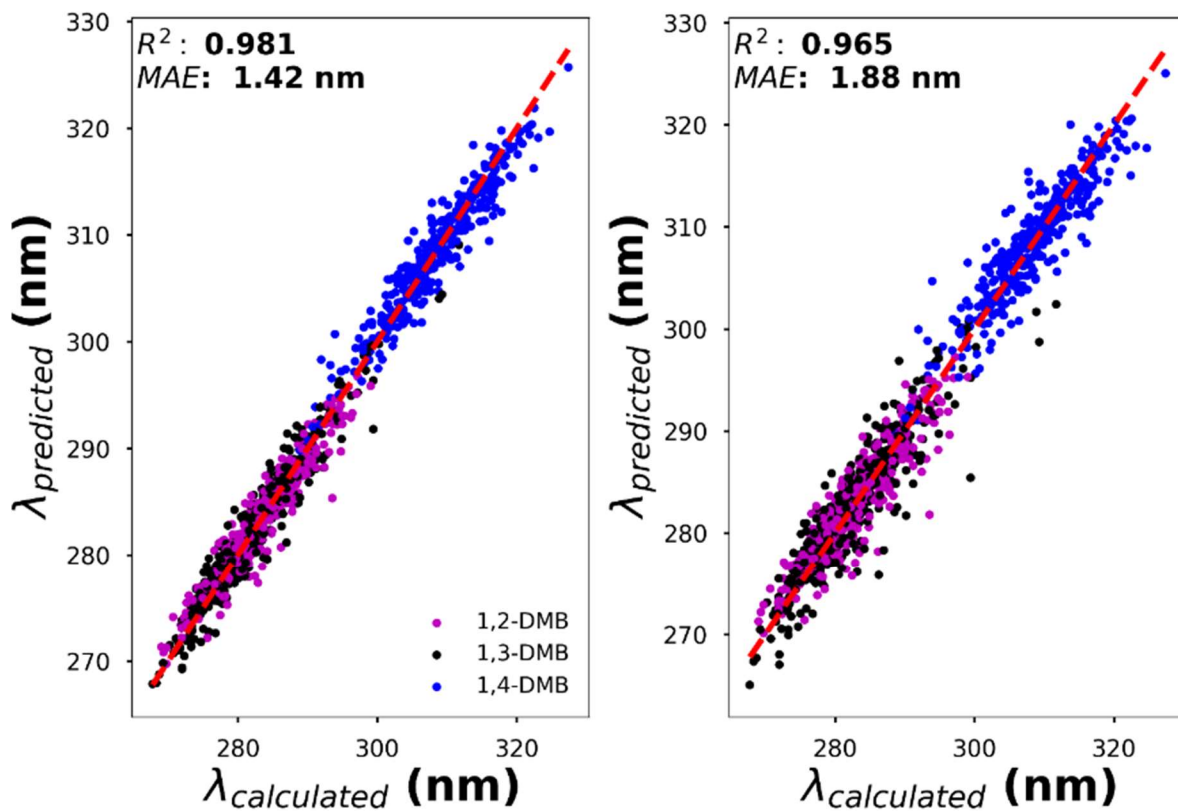


Supplemental Figure S24. Model compound absorbance spectra for various molar absorption coefficients.

Assumed absorption spectra for a Gaussian hypothetical model compound showing baseline peak height (black line, molar absorption coefficient = $3000 \text{ M}^{-1} \text{ cm}^{-1}$) and various other molar absorption coefficients (red and blue lines). The black dashed line (right axis) represents the TUV-modeled actinic flux for Summit conditions.



Supplemental Figure S25. Model compound photodegradation rate constant for various molar absorption coefficients. Predicted changes to photodegradation rate constants and photochemical lifetimes resulting from molar absorption coefficient changes for a hypothetical model compound. The solid black line shows the baseline peak height (molar absorption coefficients = $3000 \text{ M}^{-1} \text{ cm}^{-1}$), while the red and blue lines show the rate constants and lifetimes for various molar absorption coefficients and shifts.



Supplemental Figure S26. Machine learning parity plots. Parity plots for our unified machine learning model for the three DMB isomers. The R^2 and MAE are computed from the average R^2 and MAE from the 5-fold cross validation scheme. During each fold of the cross-validation scheme, a total of 888 frames were used in the training, 222 frames were used in the testing.

References

Bones, J. and E. Adams (2009). Controlling crystal habit in a small scale snowmaker. Proceedings of the 2009 International Snow Science Workshop, Davos, Switzerland.

Hullar, T., F. C. Bononi, Z. K. Chen, D. Magadia, O. Palmer, T. Tran, D. Rocca, O. Andreussi, D. Donadio and C. Anastasio: Photodecay of guaiacol is faster in ice, and even more rapid on ice, than in aqueous solution, Environmental Science-Processes & Impacts, 22(8), 1666-1677, doi: 10.1039/d0em00242a, 2020.

Hullar, T., D. Magadia and C. Anastasio: Photodegradation Rate Constants for Anthracene and Pyrene Are Similar in/on Ice and in Aqueous Solution, Environmental Science & Technology, 52(21), 12225-12234, doi: 10.1021/acs.est.8b02350, 2018.

Nakamura, H.: A new apparatus to produce fresh snow, Rep. Natl Res. Cent. Disaster Prev., 19, 229-237, 1978.

Schleef, S., M. Jaggi, H. Lowe and M. Schneebeli: An improved machine to produce nature-identical snow in the laboratory, Journal of Glaciology, 60(219), 94-102, doi: 10.3189/2014JoG13J118, 2014.

USEPA. (2021). "CompTox Chemicals Dashboard." from <https://comptox.epa.gov/dashboard/>.